THE JOURNAL OF COMPARATIVE NEUROLOGY 434:379–412 (2001)

# Layer V in Cat Primary Auditory Cortex (AI): Cellular Architecture and Identification of Projection Neurons

JEFFERY A. WINER[1]* AND JORGE J. PRIETO[2]
[1]Division of Neurobiology, Department of Molecular and Cell Biology, University of California at Berkeley, Berkeley, California 94720-3200
[2]Institute of Neurosciences, Universidad Miguel Hernández and Consejo Superior de Investigaciones Científicas, San Juan (Alicante), Spain

ABSTRACT

The cytoarchitectonic organization and the structure of layer V neuronal populations in cat primary auditory cortex (AI) were analyzed in Golgi, Nissl, immunocytochemical, and plastic-embedded preparations from mature specimens. The major cell types were characterized as a prelude to identifying their connections with the thalamus, midbrain, and cerebral cortex using axoplasmic transport methods. The goal was to describe the structure and connections of layer V neurons more fully. Layer V has three sublayers based on the types of neuron and their sublaminar projections. Four types of pyramidal and three kinds of nonpyramidal cells were present. Classic pyramidal cells had a long apical dendrite, robust basal arbors, and an axon with both local and corticofugal projections. Only the largest pyramidal cell apical dendrites reached the supragranular layers, and their somata were found mainly in layer Vb. Three types departed from the classic pattern; these were the star, fusiform, and inverted pyramidal neurons. Nonpyramidal cells ranged from large multipolar neurons with radiating dendrites, to Martinotti cells, with smooth dendrites and a primary trunk oriented toward the white matter. Many nonpyramidal cells were multipolar, of which three subtypes (large, medium, and small) were identified; bipolar and other types also were seen. Their axons formed local projections within layer V, often near pyramidal neurons. Several features distinguish layer V from other layers in AI. The largest pyramidal neurons were in layer V. Layer V neuronal diversity aligns it with layer VI (Prieto and Winer [1999] J. Comp. Neurol. 404:332–358), and it is consistent with the many connectional systems in layer V, each of which has specific sublaminar and neuronal origins. The infragranular layers are the source for several parallel descending systems. There were significant differences in somatic size among these projection neurons. This finding implies that diverse corticofugal roles in sensorimotor processing may require a correspondingly wide range of neuronal architecture. J. Comp. Neurol. 434:379–412, 2001. © 2001 Wiley-Liss, Inc.

**Indexing terms: layer 5; cerebral cortex; corticocortical; corticocollicular; corticothalamic projection cells**

A key role of the cerebral cortex is to influence subcortical centers that control rapid motor adjustments. For example, the primary motor cortex (MI) sends commands to brainstem (Kuypers and Lawrence, 1967) and spinal cord (Phillips and Porter, 1977) motoneurons that initiate voluntary action in the final common pathway. The executive corticofugal signals arise from neurons principally in layer V (Jones and Wise, 1977). The primary auditory cortex (AI) has similar connections, except that its layer V neurons have no known monosynaptic contact with lower motoneurons (Winer et al., 1998). Nevertheless, layer V neurons in AI have, much like those in MI, direct input to the striatum (Reale and Imig, 1983; Flaherty and Graybiel, 1995), thalamus (Colwell, 1975; Moriizumi and Hattori, 1991), midbrain (Diamond et al., 1969; Games and Winer, 1988; Beneyto et al., 1998), and medulla (Hallman

Grant sponsor: National Institutes of Health; Grant number: R01 DC 02319-21.

This work is dedicated to Steven A. Joseph.

*Correspondence to: Jeffery A. Winer, Division of Neurobiology, Room 289 Life Sciences Addition, Department of Molecular and Cell Biology, University of California at Berkeley, Berkeley, California 94720-3200. E-mail: jawiner@socrates.berkeley.edu

Received 10 May 2000; Revised 12 September 2000; Accepted 8 February 2001

© 2001 WILEY-LISS, INC.

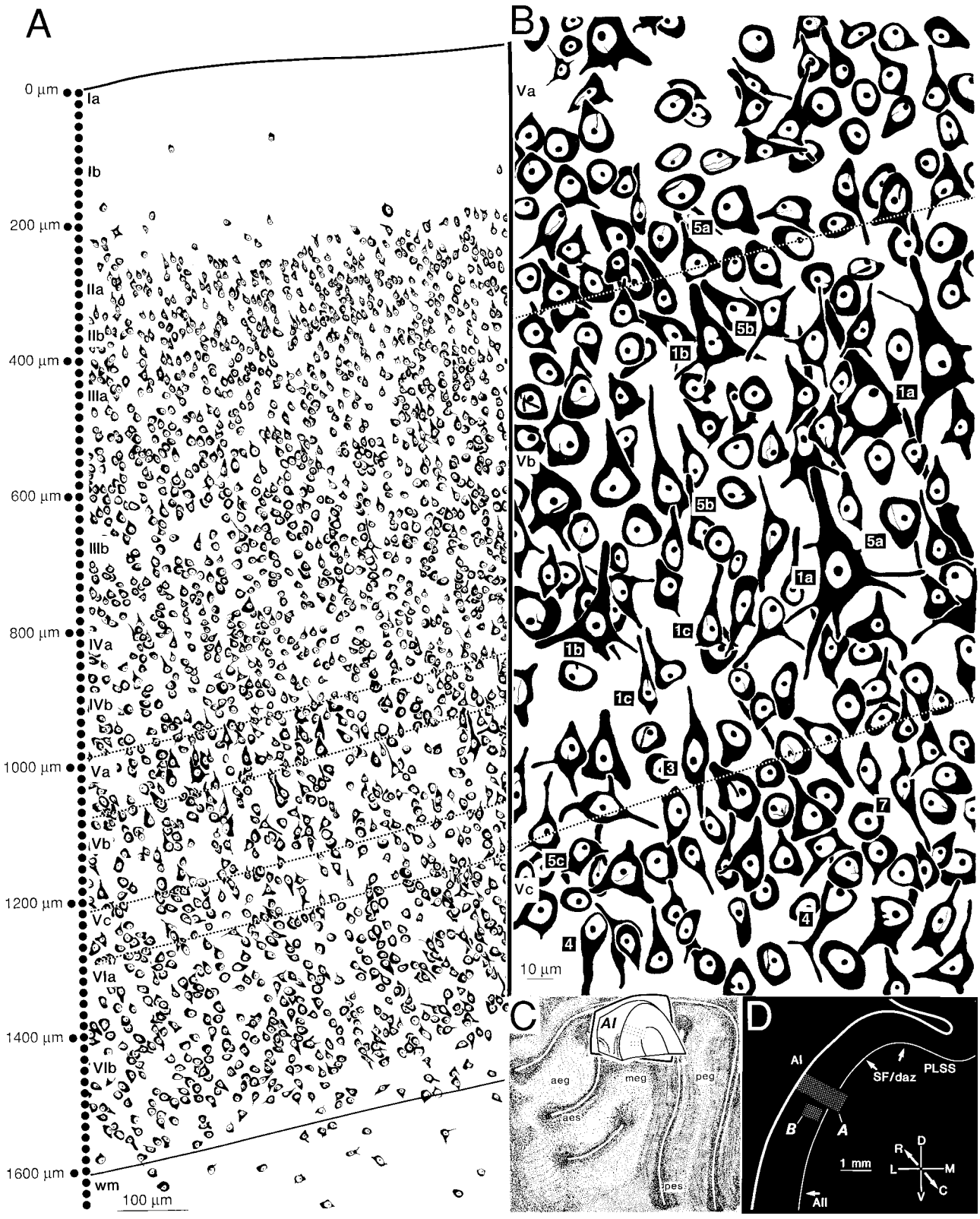


Fig. 1. Cytoarchitecture of cat primary auditory cortex (AI) and of layer V in Nissl preparations. **A:** Low-power survey from pia (0 μm) to white matter (wm) showing the laminar borders midway through AI (for orientation, see C,D). Layer I was cell-poor, with most neurons in layer Ib. Layer II cells were smaller than those in layer III and formed small clusters in layer IIa. The largest layer III pyramidal cells were in layer IIIa. Layer IV neurons were almost exclusively nonpyramidal and smaller than cells in layers III and V. The layer Va border was marked by many medium and a few large pyramidal cells; layer Va was about one-fourth the thickness of layer V. Layer Vb was almost three times as thick, with many large pyramidal cells (Fig. 4: 1a). Layer Vc was as thick as layer Va, its neurons smaller than those in layer Vb, and it had no large pyramidal cells. Layer VIa neurons were smaller and more heterogeneous than layer Vc cells, and there were many small pyramidal cells; layer VIb had many horizontal cells. Celloidin-embedded, 50-μm-thick section. Planapochromat, N.A. 0.65, ×500. **B:** Architectonic subdivisions of layer V. Layer Va had large neuropil-rich territories and a diverse population of pyramidal cells, including large (1a; see Table 1), medium (1b), small (1c), and inverted (4) subvarieties. In layer Vb, the cells were larger, and the large pyramidal cell (1a) was conspicuous; large (5a) and medium (5b) multipolar cells, and bipolar cells (7) were also present. In layer Vc, medium, fusiform (3) and inverted pyramidal (4) cells predominated. Numbers (in black boxes) refer to neurons immediately above or slightly to the right of the numeral in all figures. Protocol as in A. Planapochromat, N.A. 1.32, ×2,000. **C:** Schematic of AI in a lateral view of the left ectosylvian gyrus showing the locus of the observations in A,B; dorsal is at the top, rostral to the left. Inset, origin of A,B. **D:** Regional architectonic borders adjoining AI in a coronal section. For abbreviations in this and all subsequent figures, see list.

TABLE 1. Summary of Layer V Cell Types in Cat Primary Auditory Cortex

| Cell type | Subtypes | Sublayer/s | Somatic shape and size[1] | Number of primary dendrites | Dendritic field shape and size[1] | Figure(s) |
|---|---|---|---|---|---|---|
| 1. Pyramidal | a. Large | Vb | Triangular; 30 × 40 μm | 3–6 | Cylindrical; 600 × 1200 μm | 1B: 1a; 2B,C: 1a; 3: 1a; 4: 1a; 13A: 1a; 15A: 1a; 16A: 1a; 18: 1a |
| | b. Medium | Va, Vb, Vc | Triangular; 20 × 23 μm | 3–5 | Cylindrical; 240 × 860 μm | 1B: 1b; 2A,B: 1b; 3: 1b; 6A: 1b; 7: 1b; 8: 1b; 10: 1b; 11: 1b; 12C: 1b; 13A: 1b; 14A: 1b; 15A: 1b, 16A: 1b; 18: 1b |
| | c. Small | Va, Vb | Triangular; 16 × 17 μm | 3–4 | Vertically elongated; 200 × 500 μm | 1B: 1c; 2A: 1c; 3: 1; 4A; 7: 1c; 11: 1c; 13A: 1c; 14A: 1c; 15A: 1c; 16A: 1c; 18: 1c |
| 2. Star pyramidal | — | Va, Vb | Round; 15 × 15 μm | 4–6 | Vertically elongated; 300 × 450 μm | 5; 10: 2; 13A: 2; 14A: 2; 15A: 2; 16A: 2, 18: 2 |
| 3. Fusiform pyramidal | — | Vb, Vc | Fusiform; 22 × 40 μm | 6–7 | Fusiform; 300 × 700 μm | 1B: 3; 6: 3; 11: 3; 13A: 3; 14A: 3; 15A: 3; 16A: 3 |
| 4. Inverted pyramidal | — | Vb | Triangular; 20 × 29 μm | 4–5 | Conical (inverted); 300 × 540 μm | 1B: 4; 2A,B: 4; 6A: 4; 9: 4; 11: 4; 12C: 4; 13A: 4; 14A: 4 |
| 5. Multipolar | a. Large | Va, Vb, Vc | Oval or polygonal; 22 × 29 μm | 4–6 | Stellate; vertically elongated; 300 × 400 μm | 1B: 5a; 7: 5a; 12B,C: 5a; 19: 5a |
| | b. Medium | Va, Vb, Vc | Polygonal; 12 × 18 μm | 4–6 | Stellate 270 × 380 μm | 1B: 5b; 2A,C: 5b; 8: 5b; 12B,C: 5b; 19: 5b |
| | c. Small | Va, Vb, Vc | Round or oval; 10 × 10 μm | 5–6 | Stellate; 200 × 260 μm | 1B: 5c; 7: 5c; 12B,C: 5c; 19: 5c |
| 6. Martinotti | — | Vc | Triangular; 14 × 26 μm | 3–4 | Conical (inverted); 240 × 520 μm | 2A: 6; 9: 6; 12B,C: 6; 19: 6 |
| 7. Bipolar | — | Va, Vb, Vc | Fusiform; 18 × 35 μm | 4–6 | Vertical; poorly branched; 160 × 420 μm | 1B: 7; 2A: 7; 10: 7; 12B,C: 7; 19: 7 |

[1]Width by height.

*Abbreviations*

| | |
|---|---|
| AAF | anterior auditory field |
| aeg | anterior ectosylvian gyrus |
| aes | anterior ectosylvian sulcus |
| APt | anterior pretectum |
| AI | primary auditory cortex |
| AII | second auditory cortical area |
| BIC | brachium of the inferior colliculus |
| BSC | brachium of the superior colliculus |
| C | central nucleus *or* central part of the central nucleus of the inferior colliculus |
| CG | central gray |
| CN | central nucleus of the inferior colliculus |
| CIC | commissure of the inferior colliculus |
| CP | cerebral peduncle |
| Cu | cuneiform nucleus |
| DAS | dorsal acoustic stria |
| DC | dorsal cortex of the inferior colliculus |
| DCN | dorsal cochlear nucleus |
| DNLL | dorsal nucleus of the lateral lemniscus |
| DD | deep dorsal nucleus of the dorsal division |
| D | dorsal nucleus of the dorsal division |
| DS | dorsal superficial nucleus of the dorsal division |
| EP | posterior ectosylvian area |
| FCL | fusiform cell layer |
| IAS | intermediate acoustic stria |
| ICP | inferior cerebellar peduncle |
| IcT | intercollicular tegmentum |
| INLL | intermediate nucleus of the lateral lemniscus |
| Ins | insular cortex |
| I-IV | layers of the dorsal cortex of the inferior colliculus |
| IV | fourth ventricle |
| i-iii | small, elongated, or large gamma-aminobutyric acid-positive puncta |
| L | lateral part of the central nucleus of the inferior colliculus |
| LGB | lateral geniculate body |
| LGBv | lateral geniculate body, ventral nucleus |
| LL | lateral lemniscus |
| LMN | lateral mesencephalic nucleus |
| LN | lateral nucleus of the inferior colliculus |
| LP | lateral posterior nucleus |
| M | medial division of the medial geniculate body *or* medial part of the central nucleus of the inferior colliculus |
| MCP | middle cerebellar peduncle |
| meg | middle ectosylvian gyrus |
| ML | molecular layer |
| MLF | medial longitudinal fasciculus |
| MRF | midbrain reticular formation |
| mss | middle suprasylvian sulcus |
| MZ | marginal zone |
| OR | optic radiations |
| OT | optic tract |
| Ov | *pars ovoidea* of the ventral division of the medial geniculate body |
| P | posterior auditory field |
| PCL | pyramidal cell layer |
| peg | posterior ectosylvian gyrus |
| pes | posterior ectosylvian sulcus |
| PLSS | posterior lateral suprasylvian area |
| PRF | pontine reticular formation |
| pss | pseudosylvian sulcus |
| PvCN | posteroventral cochlear nucleus |
| Ra | raphe nuclei |
| Sa | sagulum |
| SC | superior colliculus |
| SCP | superior cerebellar peduncle |
| SF/daz | suprasylvian fringe area/dorsal auditory zone |
| Sgl | suprageniculate nucleus, lateral part |
| SN | substantia nigra |
| Spf | subparafascicular nucleus |
| SpN | suprapeduncular nucleus |
| Te | temporal cortex |
| V | ventral division of the medial geniculate body *or* ventral part of the central nucleus of the inferior colliculus |
| Vb | ventrobasal complex |
| VL | ventral lateral part of central nucleus of inferior colliculus |
| Vl | ventrolateral nucleus of the dorsal division of the medial geniculate body |
| VNLL | ventral nucleus of the lateral lemniscus |
| VP | ventral posterior auditory field |
| wm | white matter |
| I-VI | cortical layers |

Planes of section

| | |
|---|---|
| A | anterior |
| C | caudal |
| D | dorsal |
| L | lateral |
| M | medial |
| V | venoral |

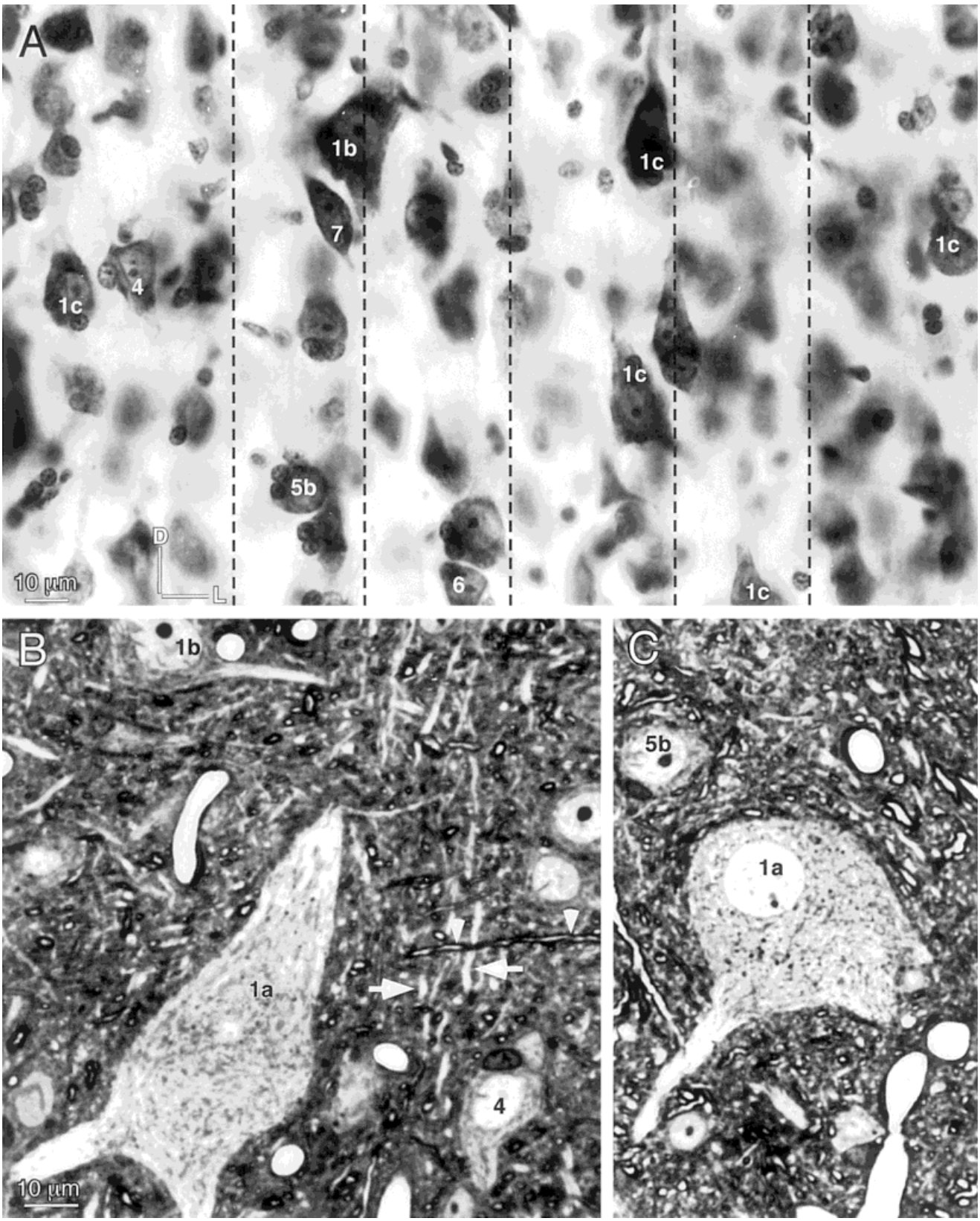


Fig. 2. Layer V cytoarchitecture and neuropil organization. **A:** Vertically oriented neuronal perikarya. Schematic borders (vertical dashed lines) denote cell- or neuropil-dominated zones in layer Va. The columns contain medium (1b), small (1c), and inverted (4) pyramidal cells and (6) a Martinotti cell. They may correspond to the columnar aggregates of cells in primate auditory cortex (von Economo, 1929; Winer, 1992). Orientation bar applies to all panels. Protocol as in Figure 1A. For A,B, Planachromat, N.A. 0.65, ×500. **B:** Neuropil arrangements near a large layer Vb pyramidal (1a) and an inverted pyramidal (4) cell in a semithin section. Pyramidal cell dendritic fascicles (large arrows) ascend with unmyelinated fibers. A thick, myelinated axon passing laterally (arrowheads) may be of pyramidal cell origin, like the equally large, oval profiles sectioned *en face*. Toluidine blue-counterstained, 1-μm-thick plastic-embedded section. Scale bar in B applies to C. **C:** A large layer V perikaryon (1a) with thick basal dendrites; a medium multipolar cell (5b) has a nuclear membrane with prominent infoldings. Protocol as in B and in Materials and Methods section.


Figure 3

et al., 1988; Weedman and Ryugo, 1996a,b). These projections arise from different sublaminae within layer V (Kelly and Wong, 1981; Killackey et al., 1989), suggesting a segregation for corticofugal processing. A further parallel is that the projection cells are exclusively pyramidal neurons (Jones et al., 1977; Weedman and Ryugo, 1996a,b) and use an excitatory amino acid neurotransmitter (Huettner and Baughman, 1988; Prieto and Winer, 1999). Moreover, in the visual cortex, these projection neurons receive fewer gamma-aminobutyric acidergic (GABAergic) axosomatic synapses than pyramidal cells in other layers (Fariñas and DeFelipe, 1991a,b; Prieto et al., 1994a,b), suggesting laminar differences in intrinsic circuitry. These many parallels between MI and AI suggest that the essential types of neurons and local circuitry differ chiefly in their peripheral input and their ultimate synaptic target. Against this proposition are the findings of different proportions of GABAergic neurons in different areas (Hendry et al., 1987) and species (Winer and Larue, 1996), which implies that processing strategies may not be identical in each system and in every species. Nonetheless, the many parallels suggest that some basic neocortical circuit elements are conserved in phylogeny.

The present study has two purposes. The first is to provide an account of layer V neuronal and cytoarchitectonic organization. Studies of auditory cortex in layers I (Winer and Larue, 1989), II (Winer, 1985), III (Winer, 1984b,c), IV (Winer, 1984a), and VI (Prieto and Winer, 1999) found a diverse set of neurons. If the neocortex contains ≈50 types of neurons (Lorente de Nó, 1938), then knowledge of their laminar distribution precedes hypotheses about their function or differences in their projections. For example, Meynert cells are absent in area AI (Sousa-Pinto, 1973b) and relatively abundant in primary visual cortex, area 17 (Chan-Palay et al., 1974), whereas the presumptively analogous Betz cells are numerous in area 4 in MI (Phillips and Porter, 1977). Such data can prompt a search for functional correlates, much as differences among pyramidal cells in apical dendritic length (Schofield et al., 1987) led to the distinction between regular spiking and intrinsically bursting corticofugal neurons (White et al., 1994; Hefti and Smith, 2000).

A second objective is to use the cell types to identify more precisely the contribution of layer V neurons to the ipsilateral corticocortical (Winguth and Winer, 1986), commissural (Code and Winer, 1985, 1986), corticothalamic (Winer, 1992), and corticocollicular (Winer et al., 1998) systems. Such data could help in subdividing layer V and in tracing the flow of information through auditory cortex, they can specify whether single types of neuron project in more than one pathway, and they can permit laminar comparisons of neuronal architecture.

## MATERIALS AND METHODS

A full account of the procedures appears in previous studies (Winer, 1984a–c; Prieto and Winer, 1999). Mature cats free of middle ear disease were used; Siamese cats or white-coated males with blue eyes were excluded. Either sodium pentobarbital (40 mg/kg, i.p.) or isoflurane (1–4%, inhalant) were administered to effect before surgery or perfusion. For surgical procedures, the anesthetic state was monitored by responsiveness to corneal and pedal stimulation. A respiratory rate of < 8/minute and pinpoint pupils were also used to assess anesthetic status. The experimental protocol was approved by the institutional animal care and use committee, and administered under veterinary supervision conforming to established guidelines (Society for Neuroscience, 1991).

### Golgi preparations

The Golgi-Cox method impregnated neurons in tissue dissected from sodium pentobarbital-anesthetized animals. The animal was chilled, and the brain was removed rapidly and immersed in potassium dichromate solution, then stored in the dark for several days (Ramón-Moliner, 1970). The blocks were sectioned serially and included material from the primary visual cortex through the somatic sensory cortex. The tissue was dehydrated in ascending alcohols, embedded in nitrocellulose, sectioned serially at 140 μm, then flattened and coverslipped. Neurons were jet black on a clear or pale background, and the impregnation revealed dendritic spines as small as ≈0.5 μm long. Axonal impregnations ranged from unsuccessful (initial segment only) to moderate (main trunk and several secondary branches) to superior (many branches impregnated in different layers, including fine terminal segments) to excellent (the preceding as well as the afferent plexus or superior impregnations of several adjacent neurons). More than 25 complete series were available.

### Histology

Plastic embedded specimens from normal animals were available. Large tissue blocks (≈4 × 6 mm) were dissected

Fig. 3 (Previous page). The three types of layer V classic pyramidal cells. 1a, Large pyramidal neurons were found principally in layer Va (Fig. 1B: 1a), among many medium pyramids (1b). They had a large soma, thickly tufted basal dendrites, and an apical process traversing several layers (see Fig. 4). 1b, The medium pyramidal cell was common throughout layer V (see also Fig. 18: 1b). The long apical dendrite had many appendages and the distal parts of the axon (not shown) had intralaminar and corticofugal projections. 1c, Small pyramidal cells were rare; their axon and the types of dendritic spines resembled the larger varieties. Neither the small nor the medium cell apical dendrite reached the pia, suggesting that input to them may differ from that of the large cell. The laminar positions were offset for illustrative purposes. The **inset** here and in Figures 4–10 shows the locus of the observation projected on a lateral reconstruction of the hemisphere (black figurine). The other inset denotes areal and laminar position of the neurons in a coronal section. Transected process are shown by a small circle at their tip. Semiapochromat, N.A. 0.95, ×1,060. Protocol for Figures 4–10: Golgi-Cox method, adult cat, 140-μm-thick section.

Fig. 4. This (1a) was the largest auditory cortical neuron (Winer, 1984a–c, 1985; Prieto and Winer, 1999). It was often in layer Vb, near the border with layer Va, in small groups or alone. The angular soma gave rise to a sheaf of basal dendrites and a single apical trunk up to 10 μm in diameter. Finer, lateral branches in layer V were up to ≈200 μm long. The apical process usually divided in layer IV or layer III, with a final tufted arbor at the base of layer I with delicate branches in layer Ia neuropil. Distal processes had many appendages, even near their branch points. The largest spines were complex and up to 10 μm long. The basal arbors were the most elaborate of any layer V pyramidal cell; their elongated, oval domain overlapped the apical system. This complexity distinguished them from medium (Fig. 3: 1b) and small (Fig. 18: 1c) pyramidal cells. The axon was 5–6 μm in diameter and did not divide near the basal processes. Planapochromat, N.A. 1.4, ×1,200.

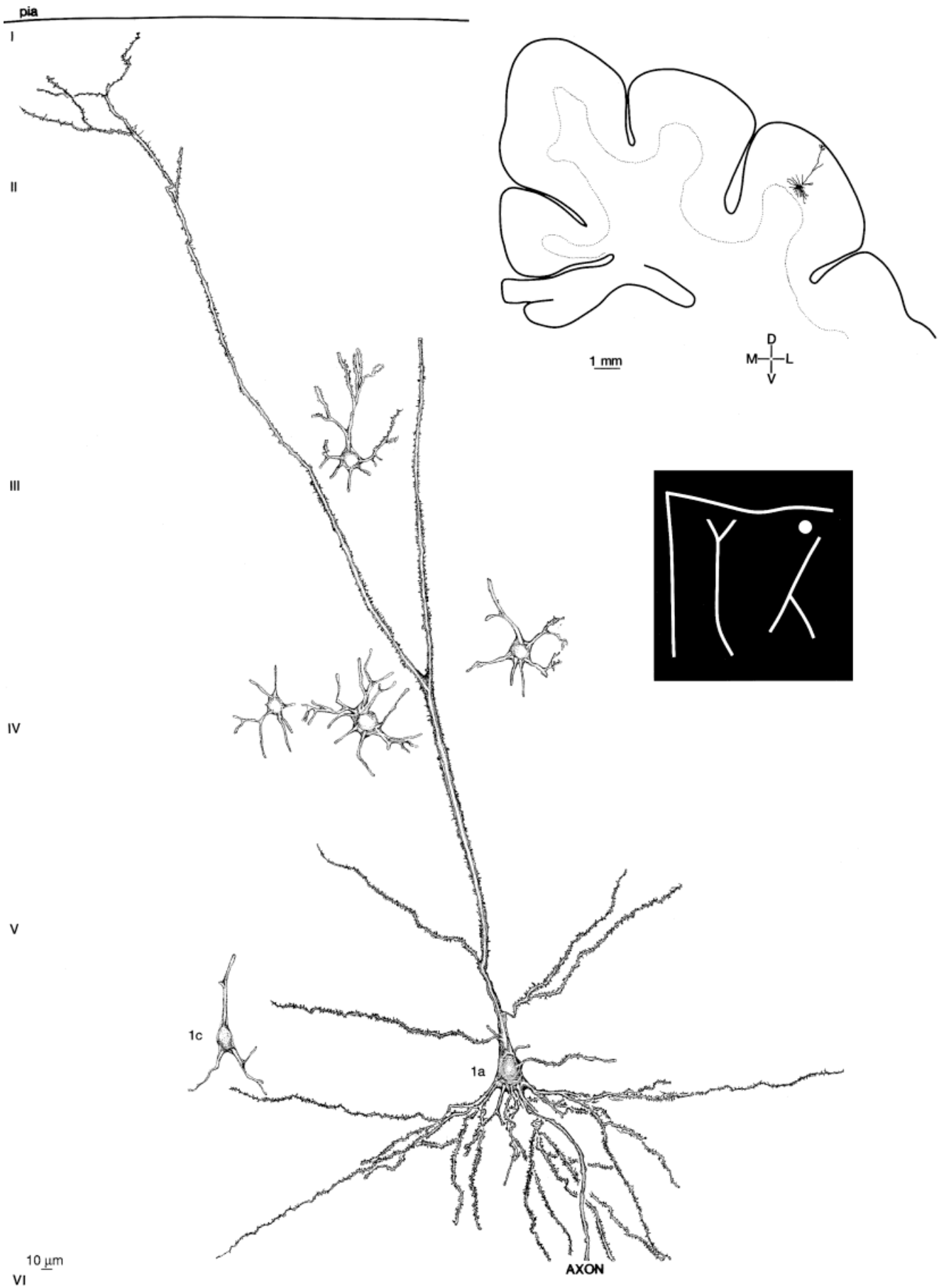


Figure 4

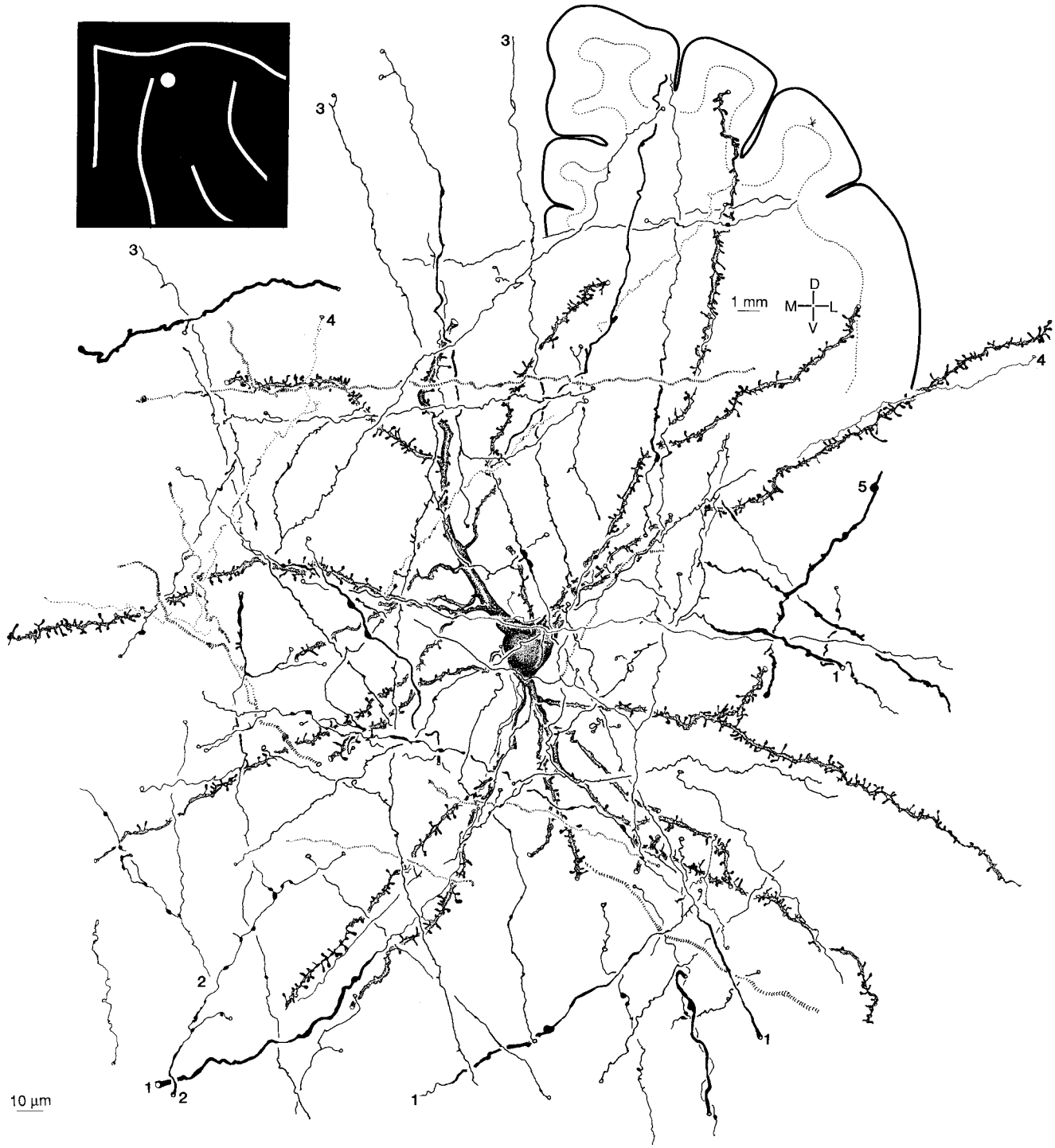


Fig. 5. Star pyramidal neuron and nearby axons. The stellate dendritic field radiated to fill a sphere. Branching was dichotomous and nonoverlapping. The apical dendrite in this and other examples (Fig. 18: 2) divided soon after its origin, projected obliquely, and usually did not reach layer I. Lateral dendrites were as thick and spinous as the apical trunk, with many appendages after the first division. 1, Thick ascending axons entered the white matter; their varicosities might represent boutons. Some axons may be of thalamic origin (Huang and Winer, 2000). 2, Fine (≈1 μm in diameter) fibers and lateral processes with boutons *en passant* resemble thalamocortical afferents (Huang and Winer, 2000). 3, Other thin fibers had fewer and smaller boutons; they may be intrinsic since they could not be followed to the white matter. 4, Delicate axons follow the dendritic contours (right side). 5, Thick (>2 μm in diameter) terminal process with large (≈4 μm) boutons; these fibers may be of cortical origin. Semiapochromat, N.A. 1.32, ×2,000.

and cut with a Vibratome (TPI, Inc., St. Louis, MO) at 50 or 100 μm and collected into cold 0.1 M phosphate buffer (PB; the vehicle in subsequent steps; pH 7.4). Slabs were osmicated for 45–90 minutes between filter paper in a Petri dish (Larue and Winer, 1996), then dehydrated in alcohols. The infiltration began with propylene oxide: Araldite and ended in 100% Araldite. The slab was placed on a cast plastic slide, covered with liquid plastic, and sandwiched between a layer of Aclar (Allied Chemical Co., Morristown, NJ) and a glass slide, then polymerized (60°C for 14–16 hours). Sections 0.5- to 1 μm-thick were cut with 8 mm-wide glass knives (LKB Ultratome III; Bromma, Sweden), annealed onto clean slides, air-dried, counterstained with 1% toluidine blue, and coverslipped. About 15 histologic series were made.

### Connectional studies

Cortical and subcortical injections of wheat germ agglutinin conjugated to horseradish peroxidase (WGA-HRP; 5% in distilled water; Sigma Chemical Co., St. Louis, MO) were made with pressure through a glass pipet affixed to a microsyringe. Tracer deposits (four 0.2-μl injections) in nonprimary auditory cortical areas (Fig. 13) and in AI (Fig. 14) labeled ipsi- and contralateral projection neurons. Tissue was processed by using conventional methods (Mesulam, 1978; Code and Winer, 1985). Eight hemispheres were available.

Auditory thalamic coordinates were chosen from a standard atlas (Berman and Jones, 1982). One or more divisions were saturated with tracer to label the corticofugal cells of origin. Twelve hemispheres with thalamic deposits were available; a representative experiment received an injection centered in the ventral division (Fig. 15; 0.15 μl).

To examine the corticocollicular projections (Fig. 16), the caudolateral part of area 17 was aspirated and the hemisphere was retracted to expose the midbrain. A pipet with a tip ≈30 μm in diameter was advanced from the rostrolateral margin of the colliculus and the WGA-HRP was ejected by using iontophoresis (1.5 μA for 30 minutes). Three experiments were available.

After a 1- to 2-day (cortical and corticocollicular experiments) or a 3-day survival period (thalamic deposits), the animal was reanesthetized and perfused. Tissue was frozen sectioned serially at 60 μm, and several series of sections were developed with tetramethylbenzidine to mark retrogradely labeled neurons, then counterstained lightly with neutral red. A separate series was prepared with diaminobenzidine, then counterstained with cresyl violet acetate to reconstruct the injection site boundaries and to determine architectonic borders.

### Data analysis and digital processing

Neuronal types were established by drawing many examples of each through a drawing tube, then classifying them with regard to somatic size and shape, dendritic branching, and axonal structure. The morphologic profile for each cell type was then compared with the somatodendritic shape and size of neurons labeled retrogradely from connectional studies (Code and Winer, 1985). Measurements (Tables 1, 2) were based on a sample of at least 10 neurons/class selected for the completeness of their dendritic trees.

Neuronal subtypes were based upon differences in somatic or dendritic size that segregate a neuron to a sublayer or which might permit interactions across sublaminae (see Fig. 17F). Thus, small pyramidal cells have somatic areas $<250$ μm$^2$, whereas the large pyramidal cells were $>900$ μm$^2$, with corresponding differences in dendritic field size that might have significance for their input. Size discrepancies between neurons in the WGA-HRP material (Fig. 17) and in Golgi preparations (Figs. 18, 19) reflect shrinkage of the WGA-HRP preparations and the extracellular deposition of the mercuric salt precipitate in the Golgi-Cox impregnations.

Digitally processed images (Fig. 2) were scanned (Nikon LS-1000, Nikon Corp.) from photographic negatives. In the final printing, lettering and symbols only were added. Standard image processing software (Photoshop, Adobe Corp., San Jose, CA) was used.

## RESULTS

AI was identified with architectonic criteria. Observations were remote from the anterior auditory field and from association areas in the posterior ectosylvian gyrus (Winer, 1992). The AI border with the suprasylvian fringe area (SF/daz) was marked by a mass of larger layer V neurons in SF/daz, while in the second auditory cortical area (AII) the granule cell layer was thinner than in AI (Winer et al., 1998).

### Cytoarchitecture

Layer V began ≈1,000 μm beneath the pia and was 350 μm thick (Fig. 1A: dashed lines). In Nissl preparations, the laminar borders corresponded closely to those in Golgi material (Winer, 1985). The definitive features of layer V relative to layer IV were the appearance of many pyramidal neurons, including the largest pyramidal cells in AI, and by a distinctive neuropil composition (see below). The layer V-VI junction had more pyramidal cell dendritic bundles in layer Vc (Prieto and Winer, 1999), a decrease in mean neuronal size (Prieto et al., 1994a, Table 3), an increased average neuronal density relative to layer IV (Prieto et al., 1994a, Table 1), and a myeloarchitecture featuring larger fascicles of axons ascending near the layer V border.

The fiber architecture of layer V was distinctive. Axons ranged in size from fascicles of 2-μm-thick, presumptive thalamocortical fibers (Huang and Winer, 2000) to larger, beaded processes with lateral branches resembling pyramidal cell local collaterals (Fig. 3: 1c). The finest fibers (Fig. 5: 3) were of intracortical origin (unpublished observations; Winer et al., 1998).

The sublaminar organization within layer V was derived from architectonic and connectional data. Three sub-

Fig. 6 (Overleaf). Fusiform pyramidal (3) and star pyramidal (Fig. 7) cells are modified pyramidal neurons; they had stellate dendritic fields, a reduced, absent, or modified apical dendrite, appendages like those of pyramidal cells, and they were glutamate immunoreactive (Figs. 11, 18: 2, black inset). **A:** The fusiform pyramidal cell's dendrites arise at the somatic poles. The tufted dendrites distinguish it from the star pyramidal cell. The axon was smaller than that of the large pyramidal (Fig. 18: 1a) or the large multipolar (Fig. 7: 5a) cells, whereas the soma was larger than that of the medium (1b) or inverted (4) pyramidal cells. **B:** The soma (inset in A) redrawn to show the nearby axons. 1–4, Fine preterminal fibers, some with delicate boutons. 5, A thicker axon near the soma. 6, A still larger fiber with perisomatic boutons. Semiapochromat, N.A. 1.32, ×2,000.

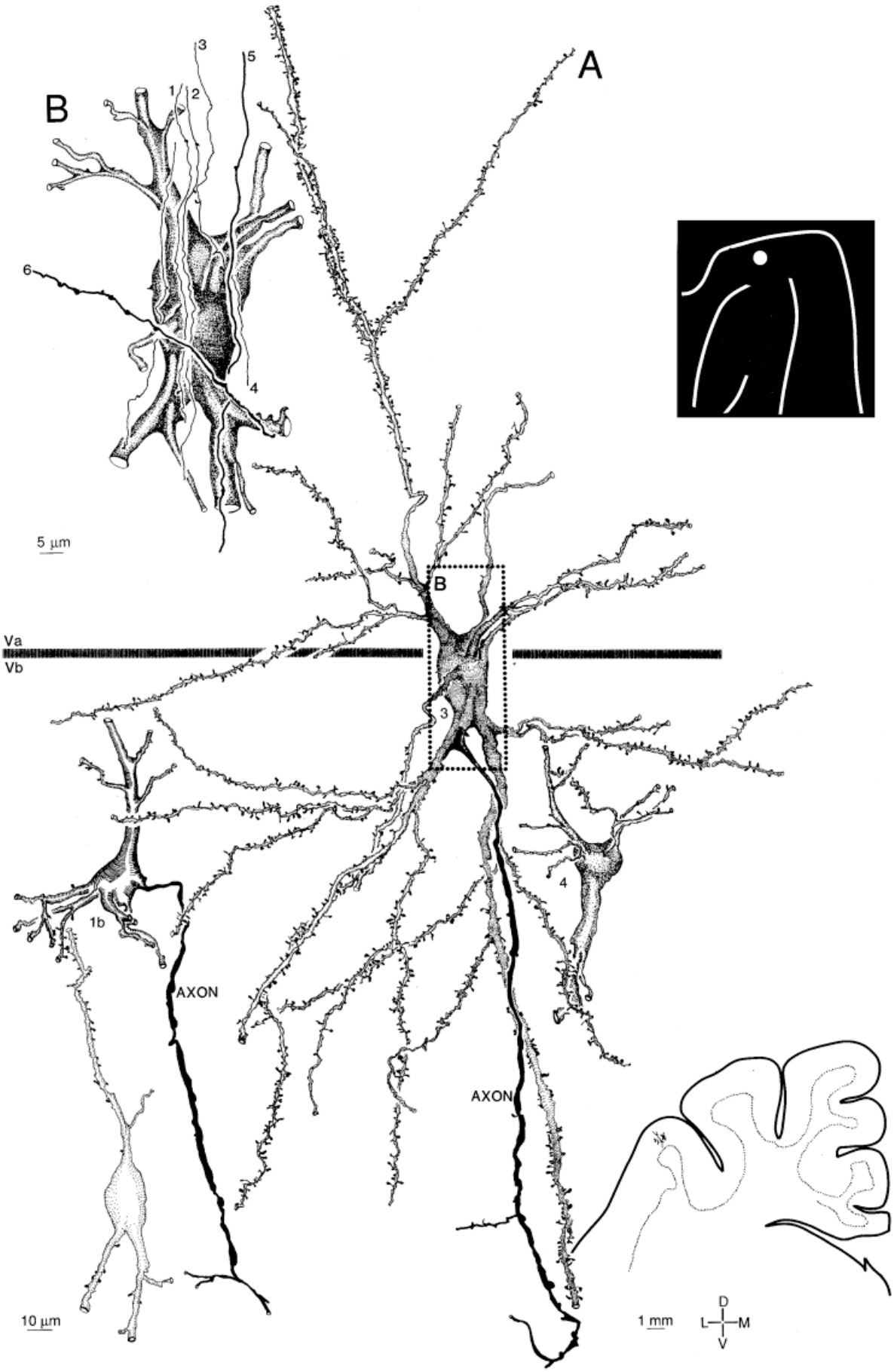


Figure 6

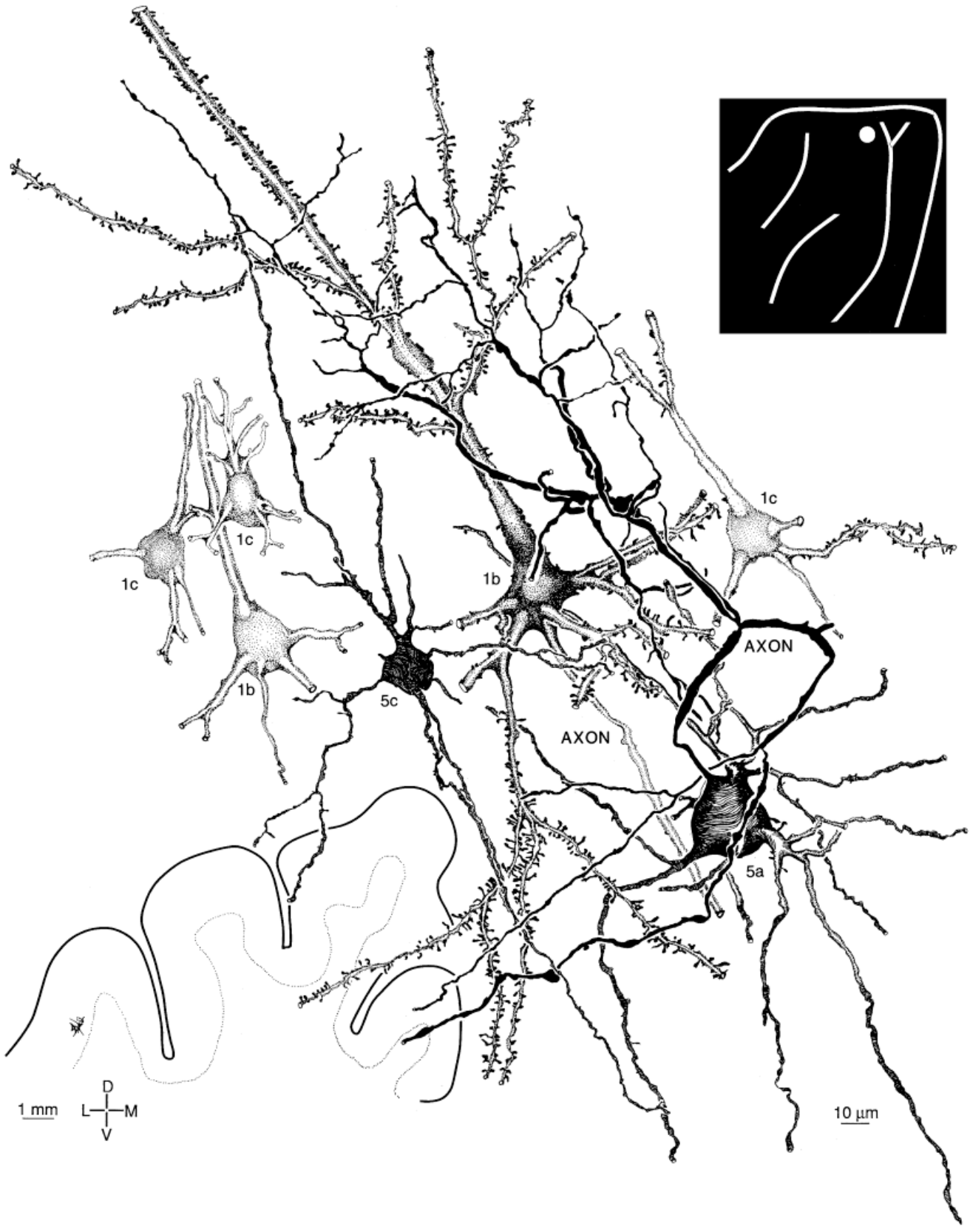


Fig. 7. Nonpyramidal and pyramidal cells in proximity. 1b (center), Medium pyramidal cells had apical and basal dendrites with various appendages. The axon arose at the somatic base and had no collateral system within the first 100 μm. A second example (left side) was similar (see also Fig. 18: 1b). 1c, Small pyramidal neurons had similar dendritic origins. 5a, Large multipolar cells were numerous and distinct from the other nonpyramidal types (Fig. 19). The axon projected near pyramidal cell somata and divided among their dendrites. Dendrites were smooth and sparsely spinous; the axon was thick, highly branched, strongly recurrent, and had boutons of different sizes. 5c, A small multipolar cell had a dendritic configuration like the larger multipolar cells. Planapochromat, N.A.1.32, ×2,000.

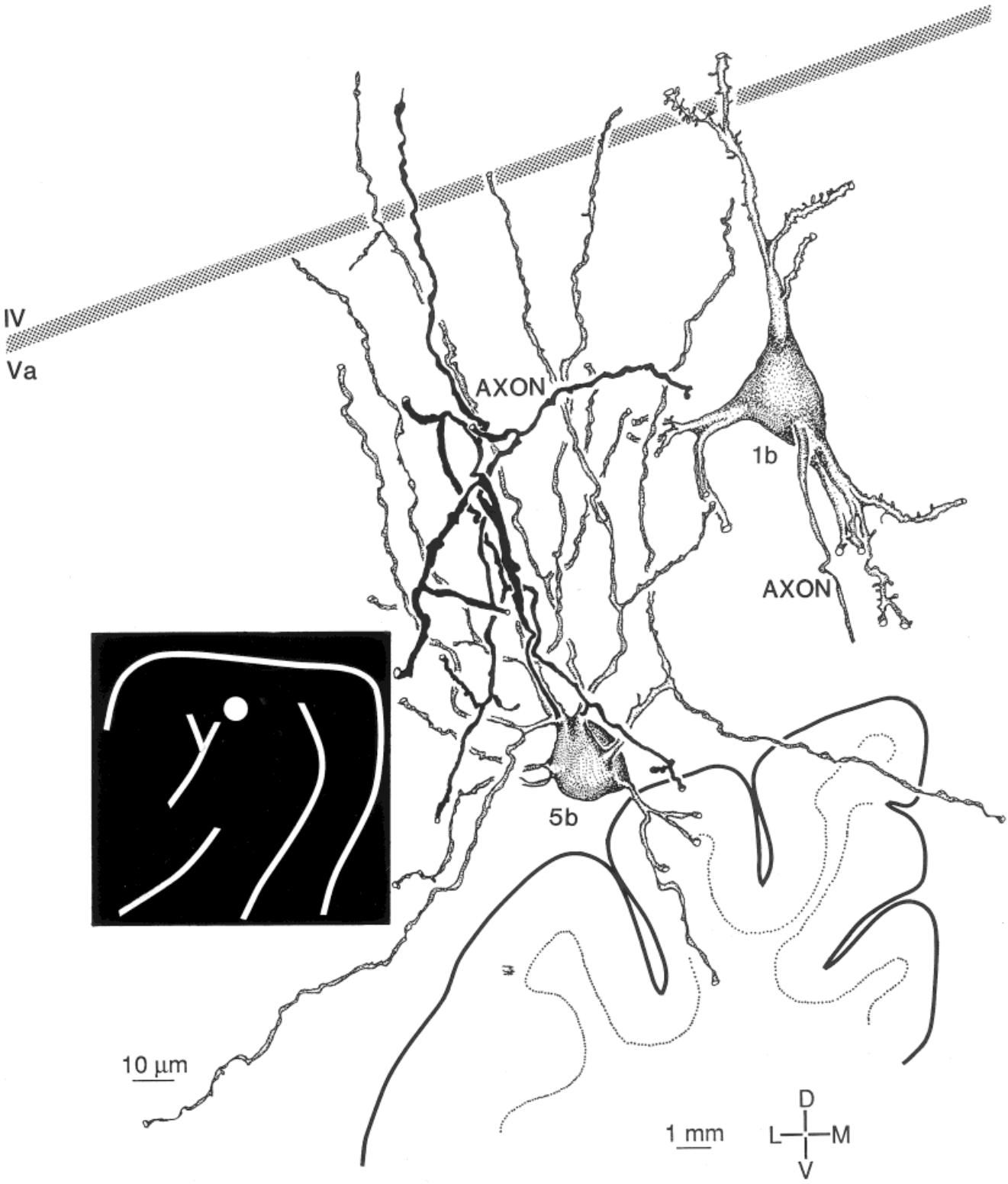


Fig. 8. The medium multipolar cell (5b) had a radiate dendritic field, thin and smooth processes confined locally, and an axon with many collaterals. The axon varied in thickness; some processes were larger than the dendrites, with swellings, constrictions, and boutons at irregular intervals. Dendritic and axonal domains overlapped, like those of most multipolar subtypes. Dendrites branched once usually and formed vertical palisades aligned with the axon. Dendrites were smooth save for occasional simple appendages ≈2 μm long. Semiapochromat, N.A. 1.32, ×2,000.

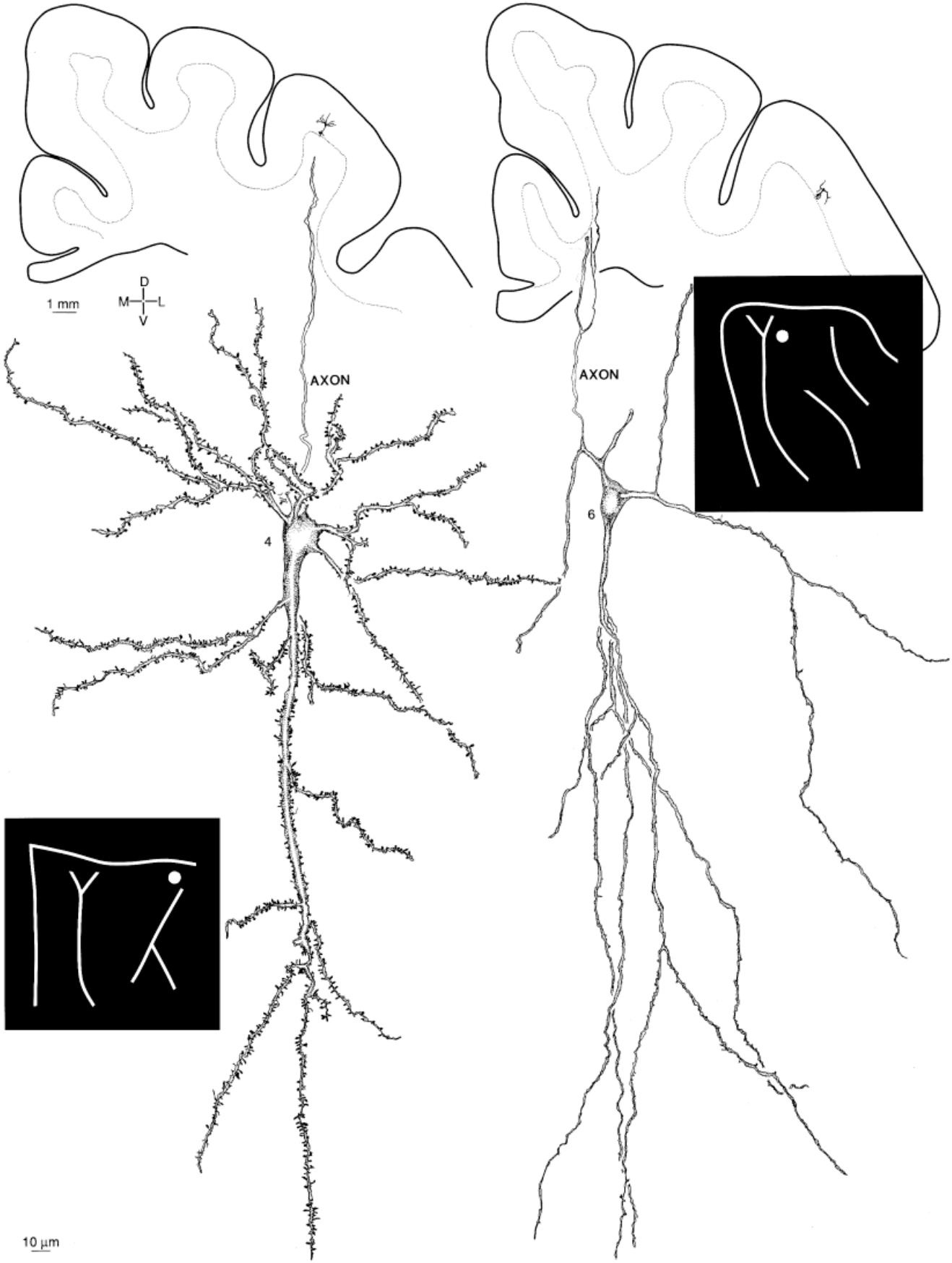


Fig. 9. Inverted pyramidal and Martinotti cells. Although their dendritic fields were similar in size, the inverted pyramidal cell (4) was much larger, with thicker dendrites and a bigger soma. They resemble the medium pyramidal cell in their dendritic configurations, in their matching axonal origins, and in their sublaminar distribution. The ventral, main dendrite of the spinous inverted pyramidal cell sometimes branched more and was shorter. The Martinotti cell (6) resembled the inverted pyramidal cell only superficially (see Results section). They had no apical (ventral) dendrite but only a sheaf of many fine processes of equal length; oblique branches were absent. The basal (dorsal) dendrites were more developed in other examples (Fig. 19: 6). This cell was sparsely spinous and GABAergic (Prieto et al, 1994a; see also Fig. 12B,C: 6). Semiapochromat, N.A. 0.95, ×1,060.

layers were recognized. Layer Va was ≈75 μm thick and contained predominantly small and medium pyramidal cells (Fig. 1B), which project in the corticocortical (Fig. 13B) and corticothalamic (Fig. 15B) systems. An occasional large pyramidal cell is found in layer Va, and none in layer Vc. Layer Vb is far thicker—about 200 μm—and had many large pyramidal cells (Fig. 1B: 1a), which often project in the corticocollicular system (Fig. 16A). Layer Vc was as thick as layer Va and had a heterogeneous neuronal population in which nonpyramidal cells were conspicuous. Layer Vc had strong corticothalamic (Fig. 15B) and corticocollicular (Fig. 16C) connections. Nonpyramidal cells lay throughout layer V, with Martinotti cells common in layers Vb,c. The largest pyramidal cells were concentrated in layer Vb, where their principal dendrites were up apparent in Nissl material (Table 1). They had abundant cytoplasm and eccentric (Fig. 2C: 1a) or centrally placed (Fig. 1B: 1a) nuclei with fewer invaginations than those of nonpyramidal cells (not shown).

Medium pyramidal cells (Table 1; Fig. 1B: 1b) were found throughout layer V. They had a more angular perikaryon and fewer primary processes than the large pyramidal cell. At the top of layer Va, these neurons were displaced by fascicles of thalamocortical axons that contribute to the neuronal dispersion at the layer Va-IVb border (Fig. 1A).

Small pyramidal cells were scattered within layer V. They had sparse Nissl substance and a thin rim of perinuclear cytoplasm; often, only their apical dendrite was stained in Nissl preparations (Figs. 1B: 1c, 2A: 1c).

Some nonpyramidal cells, such as the medium multipolar and bipolar neurons, were recognized in Nissl material. The stellate profile of the medium multipolar cell was noteworthy in thick sections (Fig. 1B: 5b), and the soma was much larger and rounder than that of the small pyramidal cells (Fig. 1B: 1c). The processes arose from the entire somatic perimeter, while the inverted pyramidal cells had only one thick dendrite in Nissl preparations, and this projected toward the white matter (Fig. 1B: 4). Bipolar cell somata were similar in size to inverted pyramidal cells (Table 1), but elongated vertically, symmetrical at the somatic apex and base, and with two thick dendrites filled with Nissl substance (Fig. 1B: 7).

## Pyramidal neurons

***Large pyramidal cells.*** These neurons had a massive dendritic field and the largest perikaryon in AI (Fig. 3: 1a; Table 1). They were concentrated in layer Vb (Fig. 1B: 1a) and dispersed in Va (Fig. 1A: Va). The triangular soma had 3–5 basal dendrites about half as thick as the apical process, which was the largest and longest in AI, and it formed elaborate local tufts in the layer Ia neuropil (Fig. 4: 1a) (Winer and Larue, 1989). This dendrite branched a few times obliquely or acutely; many processes entered layer IV. Dendritic appendages resembled those on other AI pyramidal cells (Winer, 1984b, 1985) and were ≈1–2 μm long and either solitary or in small clusters except on the second- and higher-order segments, where they were numerous.

The inferior dendrites arose at the base (Fig. 3: 1a) or from the somatic perimeter (Fig. 18: 1a). The latter origin imparted a slightly stellate appearance to the dendritic arbors of this and other pyramidal cells, which differed from those in layer III (Winer, 1984b) and resembled layer VI neurons (Prieto and Winer, 1999). Basal processes were fan-shaped and extended 200–300 μm laterally; single tufts often traveled together. The axon was 4–6 μm in diameter and acquired myelin soon after its basal somatic origin. It entered the white matter (Fig. 4: 1a, AXON) and local branches projected toward layers III and IV and perhaps beyond (not shown). All layer V pyramidal cells with a prominent apical dendrite and a corticofugal axon shared these features (Fig. 3: 1c); most pyramidal cells have remote and local projections.

***Medium pyramidal cells.*** These were the most common neuronal type in layer V, and they were present throughout its depth. They resembled the large pyramidal cells in dendritic branching, and some had apical dendrites up to 500 μm long that ended as simple tufts in layer II (Fig. 3: 1b). The lateral arbors on the apical trunk were often more elaborate than those on the large pyramidal cells (compare Fig. 18: 1a,b). The other dendrites were about half as thick as the main trunk, and they often projected irregularly from the base and lateral somatic margins. The apical process could be as thin as the basal ones (Fig. 7: 1b, left side).

Their dendritic appendages were diverse, and dendrites were increasingly spinous after their first branching point (Fig. 7: 1b, center). Most spines were simple cylinders or mushroom-shaped processes, 1–3 μm long.

The axon arose at the base of the soma and was 2–3 μm in diameter. It soon acquired myelin and entered the white matter; local branches reascended as far as layer II (not shown). Collaterals projected obliquely (across layers) or laterally (within a layer) for 200–300 μm on each side, so that their local domain might extend 500 μm.

***Small pyramidal cells.*** Like the medium pyramidal cell, these were found throughout layer V. The soma had three primary dendrites (Fig. 3: 1c). The apical process was prominent and extended ≈200 μm; it was the only layer V pyramidal cell whose apical dendrite could end in layer V. The fine basal arbors branched sparsely and dichotomously, like those of medium pyramidal cells, and they rarely formed the tufts characteristic of larger pyramidal cells. They had moderate numbers of spines after the first branch, although fewer than the medium pyramidal (Fig. 7: 1b,c) or other pyramidal cells (Fig. 6A: 3). The dendritic arbor was more weakly stellate than classically pyramidal.

The axon (Fig. 3: 1c, AXON) had both local circuit and remote projections. It issued from the ventral somatic surface and sent a 1- to 2-μm-thick trunk into the white matter. Secondary branches emerged as it descended, and these projected laterally, beyond the section. Other trunks ascended as far as layer II, while making more local branches. The axon at its origin was uniformly thick, with swellings and irregular appendages after the initial segment. Many distal axonal branches ramified among the cell's own dendrites (Lübke et al., 1996).

## Modified pyramidal cells

Three types of neuron differed so from classic pyramidal cells that they are a separate category. Each shared enough features with classic pyramidal cells—an apical dendrite, abundant dendritic appendages, a vertical orientation, a large corticofugal axon, and evidence that they are glutamatergic—to be classified as pyramidal neurons.

***Star pyramidal cells.*** Except for its thicker apical dendrite and wide lateral dendritic domain, this neuron resembled layer IV spiny stellate neurons (Winer, 1984a).

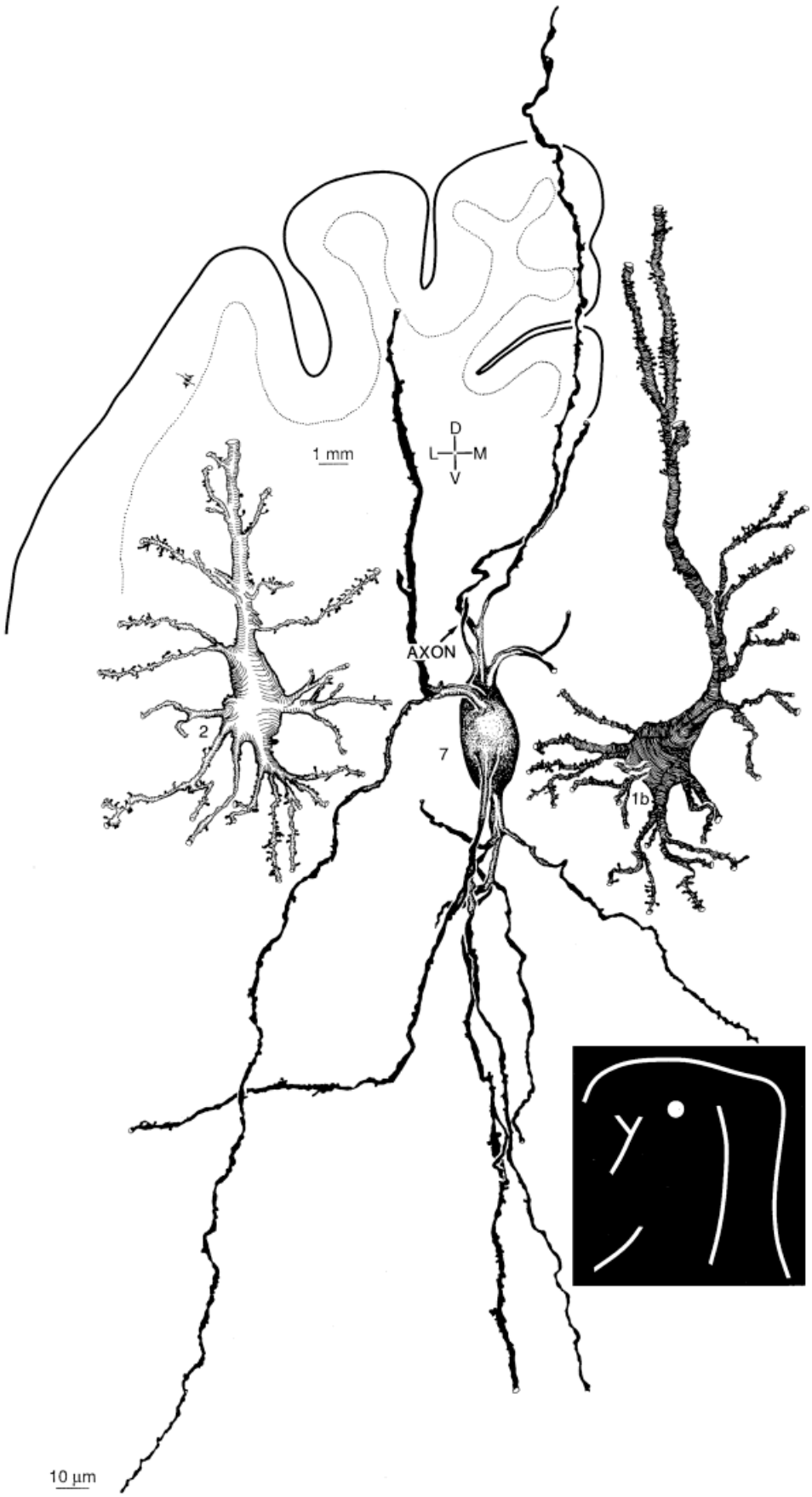


Fig. 10. Bipolar cells (7) had polarized dendritic arbors oriented vertically. Processes were sparsely spinous and of variable thickness; they divided simply or formed a tufted arbor. 1b, Medium pyramidal cell. 2, Star pyramidal cell. Semiapochromat, N.A. 1.32, ×2,000.


Fig. 11. Glutamatergic (Glu) layer V neurons. Each layer V subdivision had many Glu neurons with long immunopositive dendrites. These processes formed discrete bundles (arrows, lower left and right sides) especially in layer Va; bundles contain 3–10 parallel processes as well as dendrites from layer V and VI cells (Peters and Sethares, 1996). Dendrites from inverted pyramidal (4) or fusiform pyramidal (3) neurons may also contribute to the deeper-lying bundles. 1b, Medium pyramidal cell; 1c, Small pyramidal cell; 3, Fusiform pyramidal cell. 4, Inverted pyramidal cell. Stippled outlines, Glu-negative neurons. Monoclonal mouse antiglutamate (Madl et al., 1987), 1:20,000 dilution. Planapochromat, N.A. 1.32, ×2,000.

The denomination, star, refers to the dichotomous pattern of dendritic division, and the three-dimensional form of the dendritic field, which was spherical and radiate (Fig. 5). The soma was rounder than that of classic pyramidal cells, and the dendrites were not polarized like those of other pyramidal cell types (Figs. 3, 10: 2). The radiate and oblique dendritic field imparted a stellate profile to a neuron otherwise like pyramidal cells.

For the modest size of the soma, the apical dendrite was unusually thick. It ascended to layer IV and often projected outside the section. The apical process formed lateral dendrites soon after its origin, which contributed to the cell's unusual appearance. Secondary dendrites were straight, up to 300 μm long, and with many heterogeneous spines upon them. Appendages resembled those on classic pyramidal cells (Fig. 18: 1a–c, 2) but were more numerous and began near the soma (Fig. 5). The sparse lateral dendritic tufts also distinguished it from pyramidal cells (Fig. 18: 1a–c, 2).

The axon was rarely impregnated except at the initial segment (Fig. 18: 2, near the somatic base). It was ≈2 μm in diameter and had many local branches whose elaborate vertical plexus overlapped the dendritic domain (not shown).

***Fusiform pyramidal cells.*** This neuron was found only in layers V (Fig. 6: 3) and VI (Prieto and Winer, 1999) in AI (Winer, 1984a–c, 1992; Winer and Larue, 1989). The absence of an apical dendrite distinguished them from classic pyramidal cells (Fig. 3: 1a) and their spinous processes and unusual dendritic field set them apart from large multipolar cells (Fig. 7: 5a). They differed from medium multipolar cells (Fig. 19: 5b) by their tufted dendrites and larger size. Analogous comparisons and criteria set them apart from all other layer V neurons (Table 1).

The dendritic field was stellate, elongated vertically, and among the largest in the sample. The definitive features were two thick (≈4–5 μm in diameter), spinous dendrites at opposite somatic poles and that could span layer V.

Dendrites arose from the entire somatic perimeter and were sparsest at the lateral and central margins. The massive trunks had prominent tufts that tapered, divided progressively, and with appendages to their tips. The arbors did not overlap except distally, and the branching was stereotyped (Fig. 6, lower left). Appendages ≈1–3 μm long ranged from simple stalks to more complex profiles.

The fusiform pyramidal cell axon (Fig. 6: 3, AXON) resembled that of the medium pyramidal cell (Fig. 7: 1b, AXON). Both were 2–4 μm thick, had swellings and constrictions, lateral branches in layer Vb suggesting intracortical association projections, and a process directed toward the white matter.

***Inverted pyramidal cells.*** These neurons (Fig. 9: 4) were confined to layers V (present results) and VI (Prieto and Winer, 1999). Their correspondence with the medium pyramidal cell (Fig. 18: 1b) was striking, allowing for their unique orientation.

The elongated soma had smooth contours and ≈5 primary dendrites. Like medium pyramidal (Fig. 7: 1b), star pyramidal (Fig. 5), and fusiform pyramidal (Fig. 6: 3) cells, the dendritic field was more stellate than that of classic pyramidal cells in layers II (Winer, 1985) and III (Winer, 1984b). The inferior dendrite was thicker than the superior processes and divided dichotomously or formed branches that intermingled distally. Their planar dendritic fields were virtually intact in the depth of a section. An inferior process up to 400 μm long could reach layer VI or the white matter, whereas the superior dendrites can ascend to layer IV. Their dendrites were as spinous as those of the medium pyramidal cell (Fig. 7: 1b). After their first branch, every dendrite had many appendages, and these were varied in form.

The axon arose at the top of the soma, was 2–3 μm in diameter, and acquired myelin after leaving the dendritic territory. Examples with more extensive branching were seen, but the complete projection is unknown.

## Nonpyramidal neurons

These cells had restricted dendritic fields, smooth dendrites, and a local, usually unmyelinated, axon with intracortical projections different from those of pyramidal cells. They included many subtypes.

***Large multipolar cells.*** These neurons were found throughout layer V in Nissl (Fig. 1B: 5a), plastic embedded (not shown), and GABA (Fig 12B,C: 5a) material. They were the most numerous nonpyramidal multipolar cell.

In Golgi material their large, oval soma had a stellate dendritic configuration, and a highly branched axon (Fig. 7: 5a). An oval or oblate perikaryon with a long axis of ≈25 μm gave rise to 3–5 primary processes at approximately equal intervals. These divided and radiated 200–300 μm (Fig. 19: 5a). Dendrites had only a rare bleb or thorn, and their slightly varicose profile contrasted with that of pyramidal cell dendrites (Fig. 7: 1b).

The axon of this cell was unique. It arose from the top of the soma (Figs. 7: 5a; 19: 5a) and had horizontal and vertical projections. A primary trunk 4 μm in diameter divided into equally thick branches with many higher-order processes. Lateral branches ran parallel to medium pyramidal cell basal dendrites. Some axons were traced directly to nearby pyramidal cell somata. Recurrent branches ramified among multipolar cell dendrites. Preterminal axons were thick, varicose, and contorted, with

Fig. 12 (Overleaf). Gamma-aminobutyric acid–immunostained (GABAergic) and glutamic acid–positive decarboxylase immunostained (GAD) neurons in AI (A) and in layer V (B,C). **A:** A transverse section (for location, see C inset) showing that there are more immunopositive cells in granular and supragranular layers, larger infragranular GABAergic cells, and a wide size range in each layer. Seven sections through AI were superimposed using their blood vessels to preserve laminar registration. Planapochromat, N.A. 0.32, ×320. **B:** Representative layer V GAD-immunopositive neurons ranged from ≈10 μm (5c; small multipolar cells) to ≈25 μm in diameter (5a; large multipolar cells). Dendritic immunoreactivity extending up to 50 μm could be related to the profiles of Golgi-impregnated neurons (compare Figs. 9: 6 and 12C: 6). Some small neurons (<10 μm in diameter) had immunoreactive dendrites. 5b, Medium multipolar cells. 6, Martinotti cells. 7, Bipolar cells. Planapochromat, N.A. 1.32, ×2,000. **C:** Higher-magnification view of GAD neurons and axon terminals (puncta) spanning the depth of layer V. Neurons included all the multipolar cell types (5a–c), Martinotti cells (6), and bipolar cells (7). Puncta were uniform in density and variable in form. Most were ≈1 μm in diameter, with some up to 2 μm in diameter (i), a broad size range. Those near large multipolar cell perikarya (5a) were the largest, with a long axis of 3–4 μm, while others near medium pyramidal cells (1b) were finer. Elongated and complex terminals (ii) approach nonpyramidal cell somata, and others clustered in the neuropil (iii). Preterminal axons were followed rarely beyond the initial segment. Planapochromat, N.A. 1.32, ×2,000.

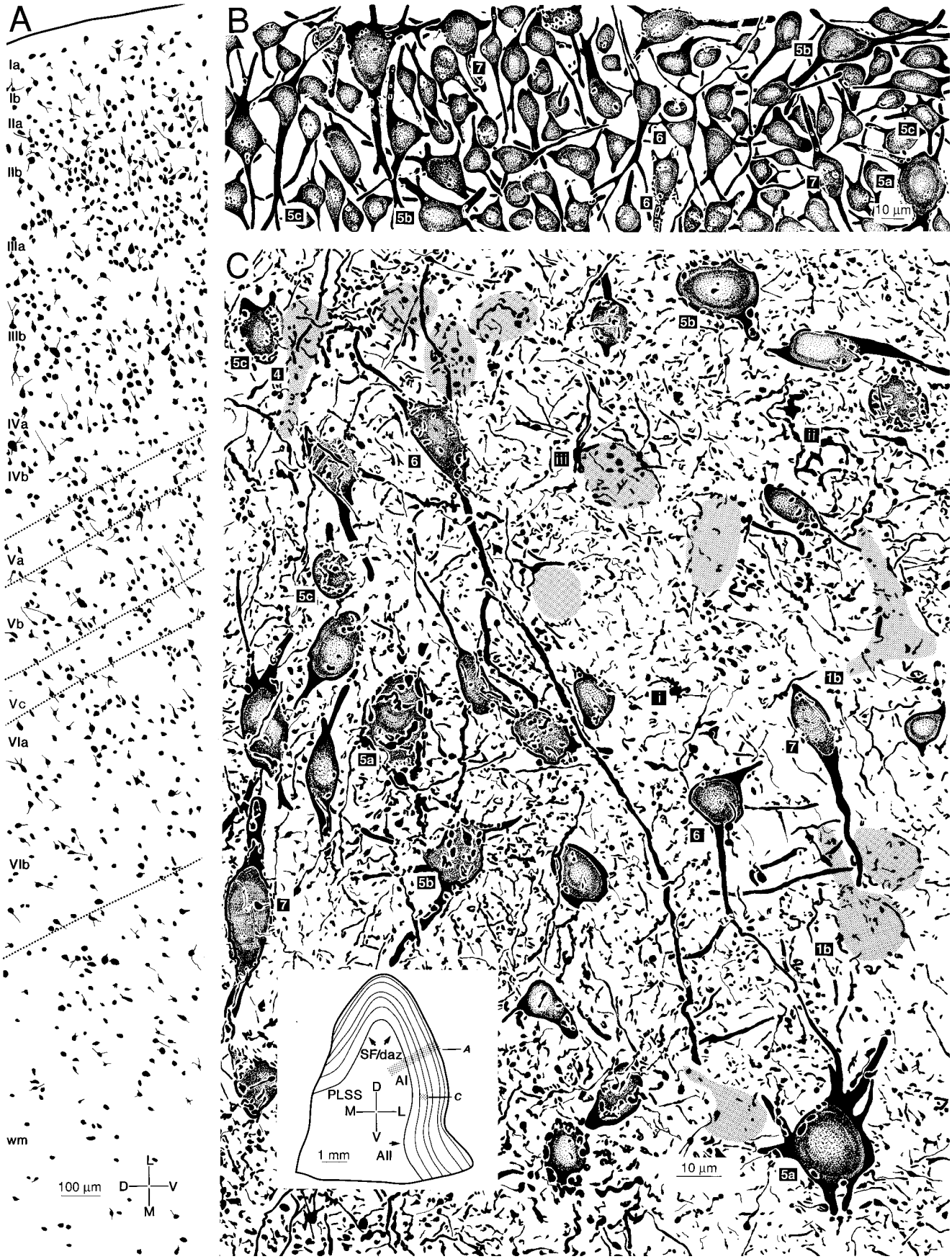
A
Ia
Ib
IIa
IIb
IIIa
IIIb
IVa
IVb
Va
Vb
Vc
VIa
VIb
wm
100 µm
L
D
V
M
B
5b
7
6
5c
5a
10 µm
C
5c
4
6
iii
5b
ii
i
1b
7
5a
6
5b
7
1c
SF/daz
A
AI
PLSS
D
c
M
L
V
1 mm
AII
10 µm
5a

Figure 12

abundant dilatations that could represent boutons. Dorsal segments were thinner with smaller boutons; these branches formed vertical palisades along pyramidal cell dendrites.

***Medium and small multipolar cells.*** These neurons (Fig. 19: 5b,5c) resembled the large multipolar cell (Fig. 7: 5a) except in somatic size. Their dendritic field was slightly larger than that of the large multipolar cell (Table 1). Common features include smooth dendrites, a spherical dendritic domain with a radiate branching pattern, few lateral processes, and an axon that arose at the top of the soma. Each class occurred throughout layer V.

Assessing the distribution of each class of multipolar cell axon was problematic since the number of completely impregnated specimens was small. All examples had an origin, size, local plexus, and branching patterns (Fig. 8: 5b, AXON) like that of the larger neuron (Fig. 7: 5a, AXON).

***Martinotti cells.*** This neuron (Fig. 9: 6) resembled the inverted pyramidal cell (Fig. 9: 4), with some important differences. These distinctions sufficed to consider it as a separate neuronal population.

The Martinotti cell had a much smaller soma and its primary dendrites were finer, straighter, and branched less than those of the inverted pyramidal cell; secondary dendritic divisions were only dichotomous. The apical dendrites were not tufted, like those of the inverted pyramidal cell; the inferior process was only slightly thicker than the superior one, and it was thinner than a true apical dendrite. Likewise, none of the most distal segments of the inferior process had a characteristic tuft. Superior dendrites were also devoid of tufts, and each was solitary, slender, and sparsely branched, with few dendritic appendages. These spines were isolated or in small clusters, usually on the secondary processes.

The axon was rarely impregnated. It arose from a superior dendrite (Fig. 9: 6, AXON), ascended vertically, and was not traced beyond layer V. Axonal trunks sometimes paralleled the dendrites.

***Bipolar cells.*** This neuron had an elongated soma and sparse dendritic arbors that were polarized vertically (Fig. 10: 7). They were similar in somatic size to the medium (Fig. 10: 1b) and star (Fig. 10: 2) pyramidal cells.

The oval perikaryon had smooth contours. At each pole, approximately three primary dendrites arose and projected toward the pia or white matter. Thin and varicose dendrites formed ascending and descending trunks along the major axis. They divided once near the cell body and filled a narrow field confined largely to the depth of the section. Dendrites had short, thorn-like appendages after their first branch point; these were $< 3$ μm long, heterogeneous in form, and clustered. The axon was impregnated too rarely to chart its distribution.

## Glutamatergic and GABAergic organization

Material immunostained for glutamate (Fig. 11) or for GABA (Fig. 12A) or its synthetic enzyme, glutamic acid decarboxylase (GAD; Fig. 12B,C) was also useful for identifying layer V and it revealed subpopulations of chemically specific neurons. For example, glutamatergic pyramidal cell apical dendrites formed fascicles within layer V (Fig. 11: arrows, lower right and left) that contributed to the columnar organization of the neuropil. There was also a significant decrease in the number of GABAergic layer V neurons relative to other layers (Prieto et al., 1994a). Glutamate immunoreactive neurons included medium and small pyramidal cells (Fig. 11: 1b, 1c), the largest pyramidal cells (Fig. 18: 1a, black inset), and fusiform (Fig. 11: 3) and inverted pyramidal (Fig. 11: 4) cells. Some apical dendrites were immunostained for 50–100 μm.

In GAD preparations (Fig. 12B,C), the dendritic immunostaining was more robust than in the GABA material (Fig. 12A). Dendritic immunoreactivity and somatic size and shape delineated each of the three types of multipolar cell (Table 1: 5a–c), Martinotti cells (Table 1: 6), and some bipolar neurons (Table 1: 7).

Puncta density was uniform across the depth of layer V, suggesting that local circuitry is cell-specific. Large axosomatic endings were apposed to large multipolar neurons (Fig. 12C: 5a), with many small and medium puncta in the neuropil (Fig. 12C: ii, iii).

## Connectional experiments

Four representative experiments involving layer V neurons show the laminar and sublaminar origins and the types of projection neuron in the ipsilateral corticocortical, commissural, corticothalamic, or corticocollicular projection, respectively. While only one example of each is illustrated, experiments were repeated 3 to 10 times. Only characteristic results are reported.

***Corticocortical projection neurons.*** Four WGA-HRP injections were centered in nonprimary auditory cortex (Fig. 13B, black inset). The deposits extended from the posterior to the anterior ectosylvian sulci but did not enter either sulcus. The cortex was saturated from the pia to the white matter and tracer diffused ≈500 μm into the white matter. The medial geniculate body retrograde labeling lay mainly in the dorsal division, especially in the dorsal (Fig. 13D: D) and deep dorsal (Fig. 13D: DD) nuclei. The pattern of the transport supports the conclusion that nonprimary areas were involved (Niimi and Matsuoka, 1979). The areal cytoarchitecture was consistent with assigning the deposits to this region (Fig. 13C, lower inset) as was

Fig. 13 (Overleaf). Layer V AI neurons projecting to ipsilateral auditory fields. **A:** Representative corticocortical neurons. In contrast to the commissural experiments (Fig. 14), which labeled five types of projection cells, this pathway involved more varieties (Table 2). Few large pyramidal cells (1a) were present, while medium (1b), small (1c), and star (2) pyramidal cells were numerous, as were fusiform pyramidal cells (3) with their elongated somata and polar dendritic origins. Inverted pyramidal cells (4) had a robust basal process and an angular soma. Numbers in Figures 13A–17A (black boxes) denote neurons immediately above or slightly to the right. Protocol for Figures 13A–16A: Planapochromat, N.A. 1.32, ×1,200. **B:** The sublaminar corticocortical origins were more diverse than those of the commissural system (Fig. 14B). Layer V was labeled through its depth, as were others except in layer I. Layers III and VI had many labeled neurons. Inset, Lateral view of architectonic fields. Protocol for Figures 13B–16B: Planapochromat, N.A. 0.32, ×125. **C:** The injection center was in layers IV–V in area Te (arrows); this locus was revised from that in a prior report (Winguth and Winer, 1986). The deposits at their maximum dorsoventral extent (black inset above). White, injection core; stippled, zone of diffusion. Protocol for Figures 13C–16C: Semiapochromat, N.A. 0.13, ×15. **D:** Thalamocortical labeling consistent with the cytoarchitectonic assignment of the injection site to area Te, with many cells in each dorsal division nucleus (DS, D, DD, Sgl), and sparse medial division (M) projections. The ventral division labeling may reflect damage to axons passing toward AI. Each dot represents one neuron. Inset, locus of B and areal borders. Protocol for Figures 13D–16D,E: Planapochromat, N.A. 0.65, ×320.

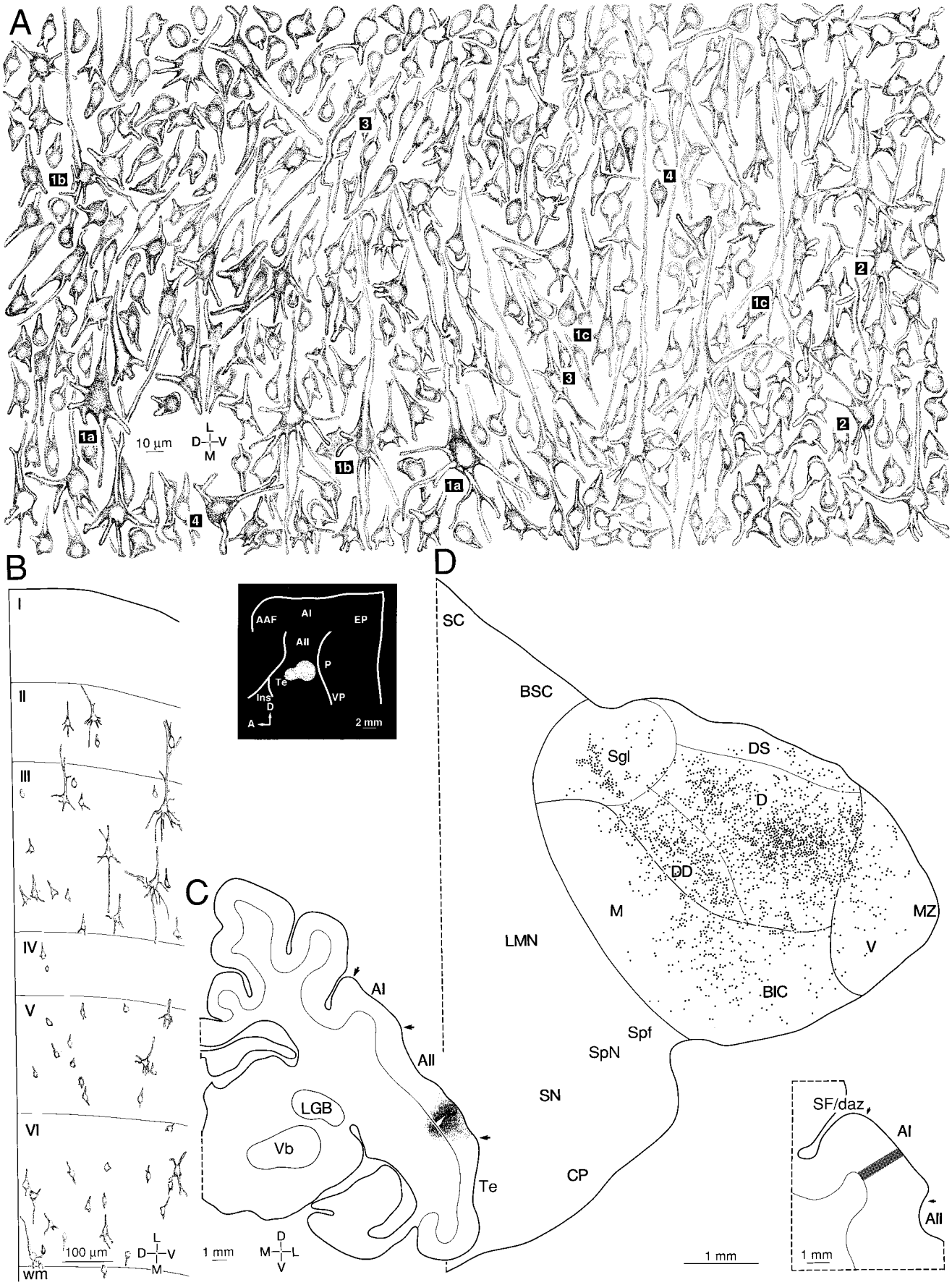
A
1b
3
4
2
1c
1c
3
2
1a
10 µm
L
D
V
M
1b
1a
4
B
I
II
III
IV
V
VI
wm
100 µm
L
D
V
M
AAF
AI
EP
AII
P
Te
Ins
VP
D
A
2 mm
C
AI
AII
LGB
Vb
Te
1 mm
D
M
L
V
D
SC
BSC
Sgl
DS
D
DD
M
MZ
V
BIC
LMN
Spf
SpN
SN
CP
1 mm
SF/daz
AI
AII
1 mm

Figure 13

the locus of the labeled cortical neurons (Rose, 1949; Winer, 1992).

The laminar distribution of AI projection neurons involved all but layer I. In layer V, these cells were found in each sublayer (Fig. 13B). Since the dendritic filling was more extensive than in the next, commissural experiment (Fig. 14A), the distinctions between the types of neurons were clearer. Medium (Fig. 13A: 1b) and small (Fig. 13A: 1c) pyramidal cells were often marked, whereas few large pyramidal neurons were labeled (Fig. 13A: 1a). Star pyramidal cells (Fig. 13A: 2) were present. Fusiform pyramidal neurons were more difficult to identify since their dendritic origins are irregular (possible examples appear in Fig. 13A: 3). Another type labeled was the inverted pyramidal cell (Fig. 13A: 4). Corticocortical (Fig. 17A) neurons had significantly smaller somata (Table 2; Fig 17C) than commissural (Fig. 17B) cells.

***Commissural projection neurons.*** Two 0.2-μl injections of WGA-HRP were made along the crest of the middle ectosylvian gyrus (Fig. 14B, black inset). Areal borders were identified subsequently in architectonic preparations (Winer et al., 1998). One deposit was at the layer VI-white matter junction, the other ≈2 mm deeper (Fig. 13C, stippled). The medial geniculate body labeling was consistent with the assignment of the injections to caudal AI, because most of the transport was in the lateral part of the ventral division (Fig. 14D: V), a region associated with the low-to-middle range frequency representation (Imig and Morel, 1984). Labeled neurons in the dorsal and deep dorsal (Fig. 14D: D,DD) nuclei may reflect damage to axons en route to nonprimary areas (Fig. 14C: SF/daz) that receive significant projections from the dorsal division nuclei (Niimi and Matsuoka, 1979; Huang and Winer, 2000).

In the contralateral AI, layers III, V, and VI (Fig. 14B) were labeled as expected (Imig et al., 1982; Code and Winer, 1985). While the layer V labeling was relatively lighter than in layer III, the large deposit labeled cells throughout AI (Fig. 14A). Those identified reliably are medium (Fig. 14A: 1b) and small (Fig. 14A: 1c) pyramidal cells, star (Fig. 14A: 2) and inverted (Fig. 14A: 4) pyramidal neurons, and fusiform pyramidal cells (Fig. 14A: 3). Few large pyramidal neurons (Fig. 4: 1a) were labeled, despite the involvement of layer Vb, where they concentrate (Fig. 1B). The medium pyramidal cells have an angular somatic profile, a prominent apical dendrite, and thinner basal dendrites (Fig. 18: 1b). It was distinguished from fusiform pyramidal cells (Figs. 6: 3, 14A: 3) since the latter had equally thick processes at their poles. In contrast, inverted pyramidal cells (Figs. 9: 4, 14A: 4) had a thick inferior main dendrite with thinner lateral processes. Somatic size, dendritic configuration, or both, excluded other plausible candidates. Small pyramidal (Fig. 14A: 1c) and fusiform pyramidal (Fig. 14A: 3) cells were common, followed by inverted pyramidal cells (Fig. 14A: 4).

***Corticothalamic projection neurons.*** These experiments support the sublaminar division of layer V because their projections arise from layers Va and Vc (as well as layer VIa). The results in this (Fig. 15) and the corticocollicular (Fig. 16) experiments differed from those in the corticocortical (Fig. 13) and commissural cases (Fig. 14): the cells of origin were mainly classic pyramidal cells with long, well-filled apical dendrites. These cells were second in labeling density only to the layer V cells projecting to the inferior colliculus (Fig. 16A). The deposit filled the central part of the ventral division (Fig. 15C: Ov) and diffused into the entire high-frequency sector (Imig and Morel, 1984), with slight involvement of the dorsal nuclei (Fig. 15C: D,DD) and the medial division (Fig. 15C: M). In the ipsilateral inferior colliculus, the central nucleus, dorsal cortex, lateral nucleus (Morest and Oliver, 1984), and subcollicular and lateral tegmental midbrain nuclei (Berman, 1968) were involved. Much central nucleus labeling was in the ventromedial part (Fig. 15D: M,V), which represents high frequencies (Merzenich and Reid, 1974). This agrees with the topographic origin of midbrain input to the thalamus (Calford and Aitkin, 1983). Extracollicular labeling may reflect projections of lateral tegmental regions projecting to the dorsal division nuclei (Morest, 1965; Henkel, 1983; Beneyto et al., 1998).

The corticogeniculate cells filled layer VI and involved sublayers Va and Vc (Fig 15B: V). Layer VI corticothalamic neurons were smaller than layer V cells (Prieto and Winer, 1999). The layer V border (Fig. 1A) was marked by the smaller layer VI cells (Prieto and Winer, 1999). Layer V projection neurons included many medium (Fig. 15A: 1b), small (Fig. 15A: 1c), and a few large (Fig. 15A: 1a) pyramidal cells. Star pyramidal cells (Fig. 15A: 2) were also present. Dendritic filling equaled that in the corticocortical experiment (Fig. 13A) and it differentiated medium (Fig. 15A: 1b) and star (Fig. 15A: 2) pyramidal cells. The latter had a round soma and dendrites that arose from the entire somatic perimeter, whereas the medium pyramidal cells had no lateral processes and a more angular somatic profile. Some neurons resembled fusiform pyramidal cells (Fig. 15A: 3).

***Corticocollicular projection neurons.*** These were the largest corticofugal neurons (Fig. 17E) and almost all were pyramidal (Fig. 16A). They were in layer V alone (Fig. 16B) in contrast to prior experiments (Figs. 13B–15B). The track traversed the dorsal cortex and ended in the central nucleus (Fig. 16C). The injection was ≈1 mm wide with a halo of diffusion in the dorsal cortex (Fig. 16C: DC). The commissural midbrain labeling (on the right side to aid comparison with the injection site) was mainly in the central nucleus (Fig. 16D: C,L), confirming physiologic (Merzenich and Reid, 1974) and connectional (Aitkin and Phillips, 1984) studies. Dorsal cochlear nucleus pyramidal cells (Fig. 16E: PCL) were labeled ipsilaterally (Oliver,

Fig. 14 (Overleaf). Layer V commissural projection cells in AI. **A:** Various cells of origin were labeled and their profiles were compared to Golgi impregnated (present results) or immunostained (Prieto et al., 1994a) layer V cells. Five types of commissural neurons occur. Medium (1b) and small pyramidal (1c) neurons were common. Star pyramidal neurons (2) were less numerous, with distinctive stellate somatodendritic profiles. Fusiform pyramidal cells (3) were plentiful. Inverted pyramidal neurons (4) had one polar ventral dendrite and two polar dorsal processes. **B:** Commissural projection cells labeled by AI injections (white dots on black inset) were concentrated in layer III. Few or no large cells were labeled, unlike the pattern after injecting the three other layer V targets (Figs. 13, 15, 16). White inset, locus of B and areal borders. **C:** Deposits entered the white matter beneath AI. Axons ascending toward the overlying suprasylvian fringe area (SF/daz) may have been damaged. **D:** Medial geniculate labeling was concentrated in the lateral part of the ventral division (V). Some dorsal division nuclei (DS,D) may project to AI, whereas other labeling (DD, Sgl) might reflect damage to axons destined for SF/daz (Winer et al., 1998). The modest medial division labeling was consistent with its projection in other studies (Niimi and Matsuoka, 1979).

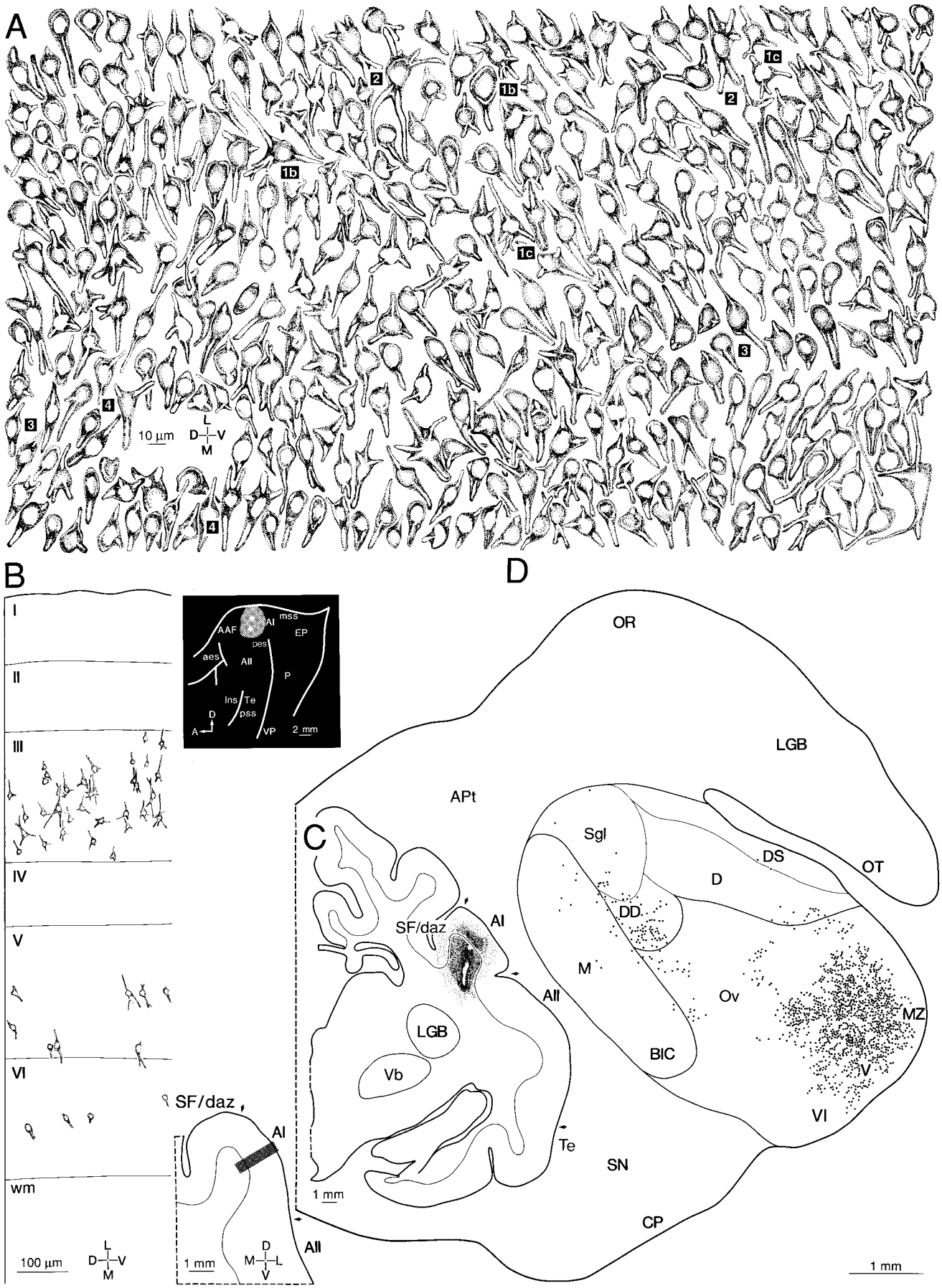
A
1b
2
1c
3
4
10 µm
L
D
V
M
B
I
II
III
IV
V
VI
wm
100 µm
mss
AAF
AI
EP
pes
aes
AII
P
Ins
Te
pss
VP
2 mm
SF/daz
AI
AII
1 mm
C
APt
SF/daz
AI
AII
LGB
Vb
Te
1 mm
D
OR
LGB
Sgl
DS
OT
D
DD
M
Ov
MZ
BIC
V
VI
SN
CP
1 mm

Figure 14

TABLE 2. Comparison of Somatic Sizes of Layer V Projection Neurons with Different Targets

| Projection system | Somatic size[1] | Median | Range | Comparison[2] | Projection types[3] |
|---|---|---|---|---|---|
| Corticocortical | 120.5 ± 35.4 | 115.5 | 52.9–236.6 | $P<0.0001$ | 1a,1b,1c,2,3,4 |
| Commissural | 150.4 ± 31.1 | 145.9 | 91.0–254.8 | | 1b, 1c, 2,3, 4 |
| Corticothalamic | 160.3 ± 62.0 | 143.6 | 59.8–431.5 | $P<0.0001$ | 1a,1b,1c, 2 |
| Corticocollicular | 305.8 ± 89.8 | 289.6 | 131.7–544.5 | | 1a,1b,1c, 2 |

[1]Mean ± standard deviation in μm.
[2]Statistical comparisons were made with Student's $t$ test, df = 199, one-tailed.
[3]See Table 1 for the classification of neuronal types.

1984). Corticocollicular neurons occupied the part of layer V nearly devoid of corticothalamic retrograde labeling (compare Figs. 15B, 16B). Medium pyramidal cells (Fig. 16A: 1b) were plentiful, followed by the small pyramidal cells (Fig. 16A: 1c). Possible star pyramidal cells were also seen (Fig. 16A: 2). Unlike the commissural labeling (Fig. 14A), most corticocollicular neurons had dendritic labeling up to 150 μm or more (Fig. 16A: 1b).

## DISCUSSION

We consider five interrelated themes. First, we assess the evidence for sublaminar organization within layer V and the functional implications that might follow. Second, how many classes of neuron exist, and how do they relate to intrinsic and extrinsic organization? Third, how do layer V anatomical arrangements compare with those in other layers? Do the connections of layer V cells offer clues to their function? Finally, why are there so many pyramidal cell subtypes?

### Sublaminar organization

Layer V was divided into three sublayers on the basis of its cytoarchitecture and its sublaminar connectivity. Layer IV in macaque striate cortex has sublayers with a distinct cytoarchitecture (Lund, 1973), unique thalamic inputs (Hubel and Wiesel, 1972), and specific cytochemical properties (Hübener and Bolz, 1992). Even in layer I, which is often regarded as devoid of sublaminar organization (see Marín-Padilla, 1984), there is sublamination since most of the neurons reside in layer Ib (Winer and Larue, 1989), because thalamic (Huang and Winer, 2000) and commissural (Code and Winer, 1986) projections target preferentially the superficial half, and there is a significant difference in the number (Prieto et al., 1994b) and qualitative (Winer and Larue, 1989) distribution of GABAergic axon terminals (puncta) within it. Differences in other layer V attributes may have functional consequences. For example, the largest neurons are found midway through layer V. This agrees with the origin of large corticothalamic axons labeled after layer Va tracer deposits and the smaller and more numerous axons from layer VI in AI (Ojima, 1994). The corticothalamic system may not be unitary either in its laminar origins (Kelly and Wong, 1981) or in the configuration of its axon terminals (Winer et al., 1999).

The corticothalamic (Fig. 15) and corticocollicular (Fig. 16) systems have separate sublaminar origins in layer V (present results). They arise from different layer V sublaminae (Figs. 15B, 16B), and collectively, they fill layer V. The sublaminar proximity of the projection neurons in different systems may allow their intracortical axon collaterals to influence other neurons. Analogous visual cortex circuitry may contribute to the augmenting response (Ferster and Lindström, 1985), and the corticothalamic system might influence thalamocortical plasticity (Castro-Alamancos and Connors, 1996). Perhaps the sublaminar origins of the corticofugal systems coordinates the discharges of inferior colliculus and medial geniculate body neurons. The larger corticocollicular neurons (Table 2) with thicker axons might compensate for the spatiotemporal offset between the auditory midbrain and thalamus, intervals that would presumably require fine intracortical timing. The large corticofugal neurons may influence motor-related functions that place conduction velocity at a premium. Since many midbrain targets have a premotor function (Huffman and Henson, 1990), a rapid input is not unexpected. The neurons projecting in these systems are similar (Table 2), although their relative proportions differ, with few large pyramidal cells projecting to the thalamus (Figs. 15A, 17D), whereas the corticocollicular neurons were nearly twice as large (Figs. 16A, 17E).

These proportions may reflect different contributions to auditory processing (Knudsen and Brainard, 1995). The inferior colliculus may make a significant nonauditory contribution to perception since many axons from nonprimary cortex target the lateral nucleus and dorsal cortex (Winer et al., 1998). The many targets of layer V corticofugal projections challenge the idea that an area, a layer, a sublayer, a cell type, or a projection has one task only (King, 1995; Weinberger, 1997; Kilgard and Merzenich, 1998).

Layer V visual corticofugal neurons project to the midbrain, the pons, or both. Evidence for specific rules of connectivity in rodent layer V projections is that these neurons do not send collaterals to the thalamic reticular

Fig. 15 (Overleaf). Layer V neurons projecting to the medial geniculate body. *A:* In contrast to the prior experiments (Figs. 13, 14), only five types of layer V neuron, all of which were pyramidal, were labeled. The dendritic labeling in this and the next (corticocollicular; Fig. 16) experiment was the most extensive, up to 200 μm. The large pyramidal cells (1a) matched the Golgi-impregnated examples (Figs. 3,4: 1a), as did other classic pyramidal cells (Fig. 3: 1b,1c); these had less dendritic labeling. Star pyramidal neurons (2) were difficult to discern. Medium (1b) and small (1c) pyramidal cells were labeled often by thalamic deposits, and large (1a), star (2), and (3) fusiform pyramidal cells far less often. **B:** Corticothalamic neurons differ from corticocortical (Fig. 13) and commissural cells (Fig. 14) in their layers of origin and sublaminar distribution. Inset, Locus of B and areal borders. **C:** The large injection was in the lateral (V) and medial (Ov) parts of the ventral division and involved the dorsal division (D) slightly; caudally, the track damaged it extensively. **D:** All inferior colliculus divisions had many retrogradely labeled cells, especially the ventromedial central nucleus (C, M), whose input to the ventral division of the medial geniculate body (Calford and Aitkin, 1983) matches auditory thalamic tonotopic organization (Aitkin and Webster, 1972). Dorsal cortex labeling involved layers III and IV preferentially.

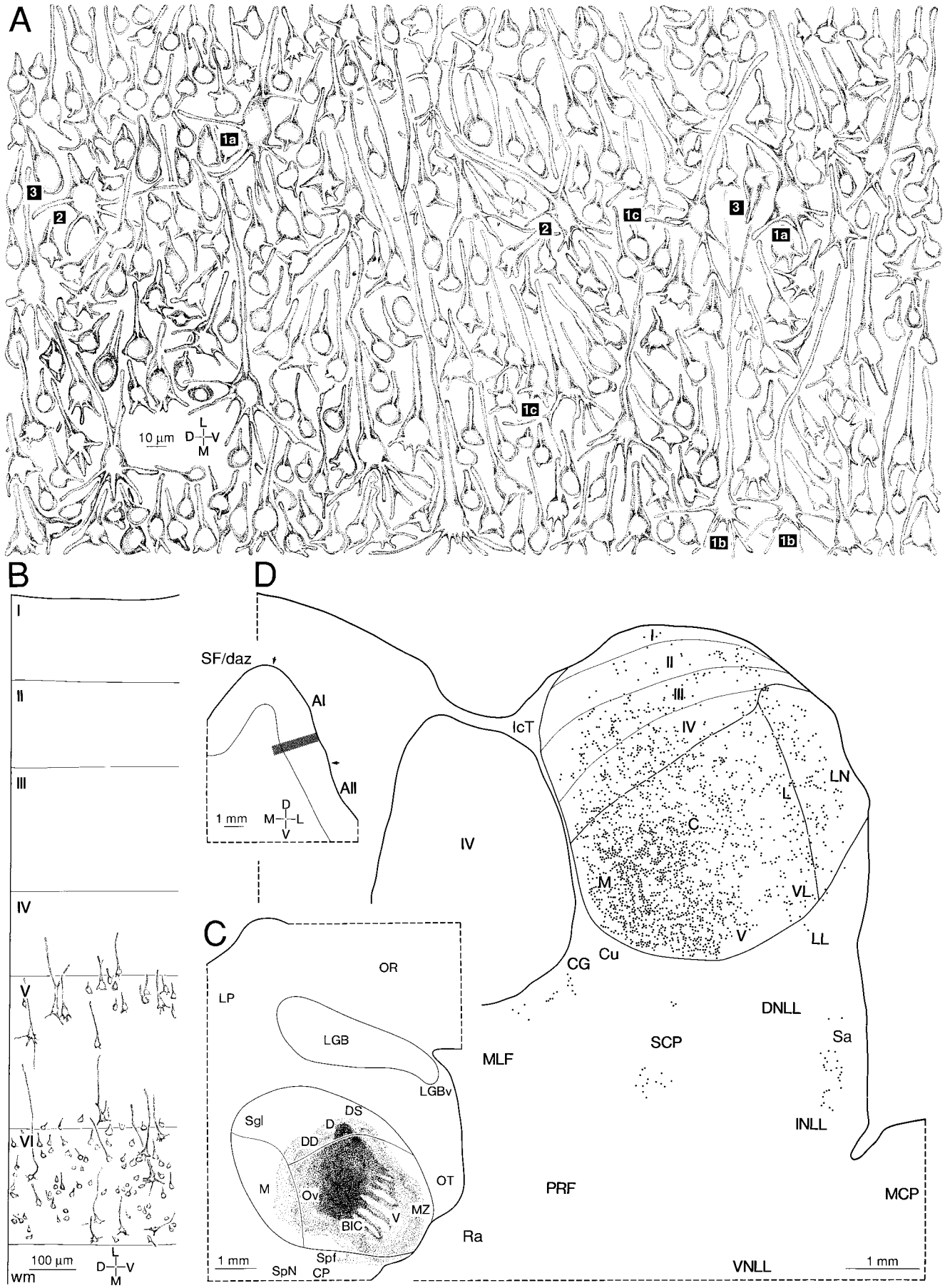
A
1a
3
2
1c
10 µm
L
D
V
M
1b
B
I
II
III
IV
V
VI
100 µm
wm
D
SF/daz
AI
AII
1 mm
M
L
V
IV
IcT
I
II
III
IV
LN
L
C
M
VL
V
LL
CG
Cu
C
OR
LP
LGB
LGBv
Sgl
DS
D
DD
M
Ov
OT
MZ
V
BIC
Spf
SpN
CP
1 mm
MLF
DNLL
SCP
Sa
INLL
PRF
MCP
Ra
VNLL
1 mm

Figure 15

nucleus, although they project widely to the thalamus and the brainstem (Bourassa and Deschênes, 1995). In cat auditory cortex, layer V projections to the thalamic reticular nucleus (Ojima et al., 1992) suggest a species specific difference in descending control. Similar patterns of axonal divergence and connectional selectivity in rodent cortex suggest parallels in layer V organization in much of the neocortex (Lévesque et al., 1996a,b). Likewise, each sublayer in layer VI of visual cortex has different subcortical targets (Fitzpatrick et al., 1994), and layer VI in AI has equally specific sublaminar patterns of corticocortical, commissural, and corticothalamic projections (Prieto and Winer, 1999). This supports the principle of finer sublamination in the corticofugal layers.

## Classification of layer V neurons

Perhaps the present scheme divides a continuum of neuronal types into classes when a broad segregation into pyramidal and nonpyramidal cells would suffice (Figs. 18, 19). The evidence against the latter idea reflects distinctions between neurons which, if valid, must have functional implications. Thus, the apical dendrite of the small pyramidal cell in layer V do not reach layer I, and most of these processes remain in layer III, whereas the large pyramidal cell apical dendrite branches robustly in layer Ib. Similarly, the small pyramidal cell axon has a more restricted local plexus than that of the large pyramidal cell, and the small pyramidal cells are an important part of the commissural system, whereas the large layer V pyramidal cells are not (Table 2). Factors besides size may distinguish neuronal subclasses. Parallels in structure and connectivity suggest that the small and large pyramidal neurons are related, despite differences in their connections. The same case can be made for the small and large multipolar neurons, although they differ in their projections and the types of neuron they target within the cortex is unknown. In visual cortex (area 18), the large basket cells have lateral projections that might contribute to intracortical disinhibition (Kisvárday et al., 1993). Perhaps the subclasses of putative basket cells in layer V in AI are matched by size with their postsynaptic neurons, for example, small basket cell to small pyramidal cell, and so forth, or basket cell-to-basket cell-mediated disinhibition may be size-matched. In vitro studies of layer V pyramidal cells find few that are interconnected beyond 150 μm, indicating that their feedforward effects are as specific, and perhaps even more focal, than those of basket cells (Nicoll and Blakemore, 1993). On the other hand, corticothalamic axons may contribute to several functional subsystems since their local axon collaterals are presynaptic to both cortical GABAergic and non-GABAergic neurons (Staiger et al., 1996).

Table 3 integrates the present scheme of classification with other, prior analyses of layer V neurons in different species and areas using the Golgi and other methods. Even among neuronal types, which might be confounded readily—such as the inverted pyramidal (Table 3: 4) and Martinotti (Table 3: 6) cells, there is remarkable unanimity of opinion over more than a century on the criteria distinguishing them. Whether the multipolar cell subtypes are distinct categorically on grounds of connectivity and neurochemistry or rather represent a continuum (Stevens, 1998) is unknown.

In prior Golgi studies in AI (Sousa-Pinto, 1973b; Winer, 1984a–c, 1985; Prieto and Winer, 1999), the main problem in classifying neurons pertains to nonpyramidal neuronal subvarieties such as clutch, spiny stellate, and chandelier cells. Clutch cells are common in layer IVC in visual cortex (Kisvárday et al., 1986), spiny stellate cells provide association connections in area 18 (Meyer and Albus, 1981), and chandelier cells are seen in the temporal cortex in young cats (De Carlos et al., 1985). We could not identify these subclasses (Table 3; Fig. 19), since the limited axonal impregnations in our mature specimens did not distinguish among small and medium multipolar neurons. Such neurons were not seen in layer V in AI in a large sample of intracellularly filled and physiologically characterized neurons; perhaps they are too small to be so labeled or too rare to be impaled often (Mitani et al., 1985).

## Connections of layer V cells

Although layer V receives input from layer VI, not all layer VI pyramidal cells project to layer V. In cat visual cortex layer VI pyramidal cells projecting to the lateral geniculate body send axon collaterals to layer IV, whereas layer V input arises from layer VI pyramids that project to the claustrum (Katz, 1987). Intrinsic inputs may reflect the extracortical target of the projection neurons in other layers. If connectivity is a definitive criterion there may be many more cell types.

Sometimes there is a correspondence between cortical neuronal morphology, physiologic properties, and projections. In hooded rat area 17, layer V corticotectal cells lie midway through the upper part of the layer, and their apical dendrite ends in layer I (Hallman et al., 1988). In contrast, the apical dendrite of layer V callosal neurons extends beyond layer IV (but not so far as those of corticotectal neurons), and these cells are more widely distributed within layer V. Thus, hooded rat corticotectal cells resemble the cells classified here as large pyramidal cells, whereas the callosal neuron types include medium, small, and fusiform pyramidal cells. Cat visual corticotectal cells follow this pattern, and some corticocortical neuron apical dendrites may not reach layer I (Hübener et al., 1990). Corticocortical cells included medium, star, and fusiform pyramidal types. Corticotectal cells in upper layer V project more strongly to the supragranular layers, whereas those in lower layer V sent more collaterals to layer VI. The local axon collaterals of corticocortical cells end mainly in layers IV, V, and VI. Large pyramidal cells may not be exclusively corticotectal because, in cat pri-

Fig. 16 (Overleaf). Projection from layer V in AI to the inferior colliculus. **A:** These neurons had substantial dendritic labeling, like the corticothalamic cells (Fig. 15). Large (1a) and medium (1b) pyramidal cells predominated. Large pyramidal cells were only in central layer V (B: V). Small pyramidal cells (1c) were numerous considering the remoteness of this target. Some star pyramidal cells (2) may be labeled. A thick apical process and radiating dendritic field arose from a distinctive perikaryon. **B:** The corticocollicular laminar origin was in central layer V; layers Va (upper part) and Vc contain corticothalamic neurons (Fig. 15B). Inset, locus of B and cortical architectonic borders. **C:** The deposit was in layers II–IV of the dorsal cortex (DC; see D) and in the middle of the central nucleus (CN), with diffusion in the intercollicular tegmentum (IcT) and dorsal cortex. **D:** The retrograde labeling in the contralateral inferior colliculus mirrored the effective injection site. Scale in D applies to E. **E:** Cochlear nucleus labeling lay mainly in the low-frequency part of the dorsal cochlear nucleus (DCN) (Spirou et al., 1993). Pyramidal cell layer (PCL) and fusiform cell layer (FCL) neurons were also labeled.

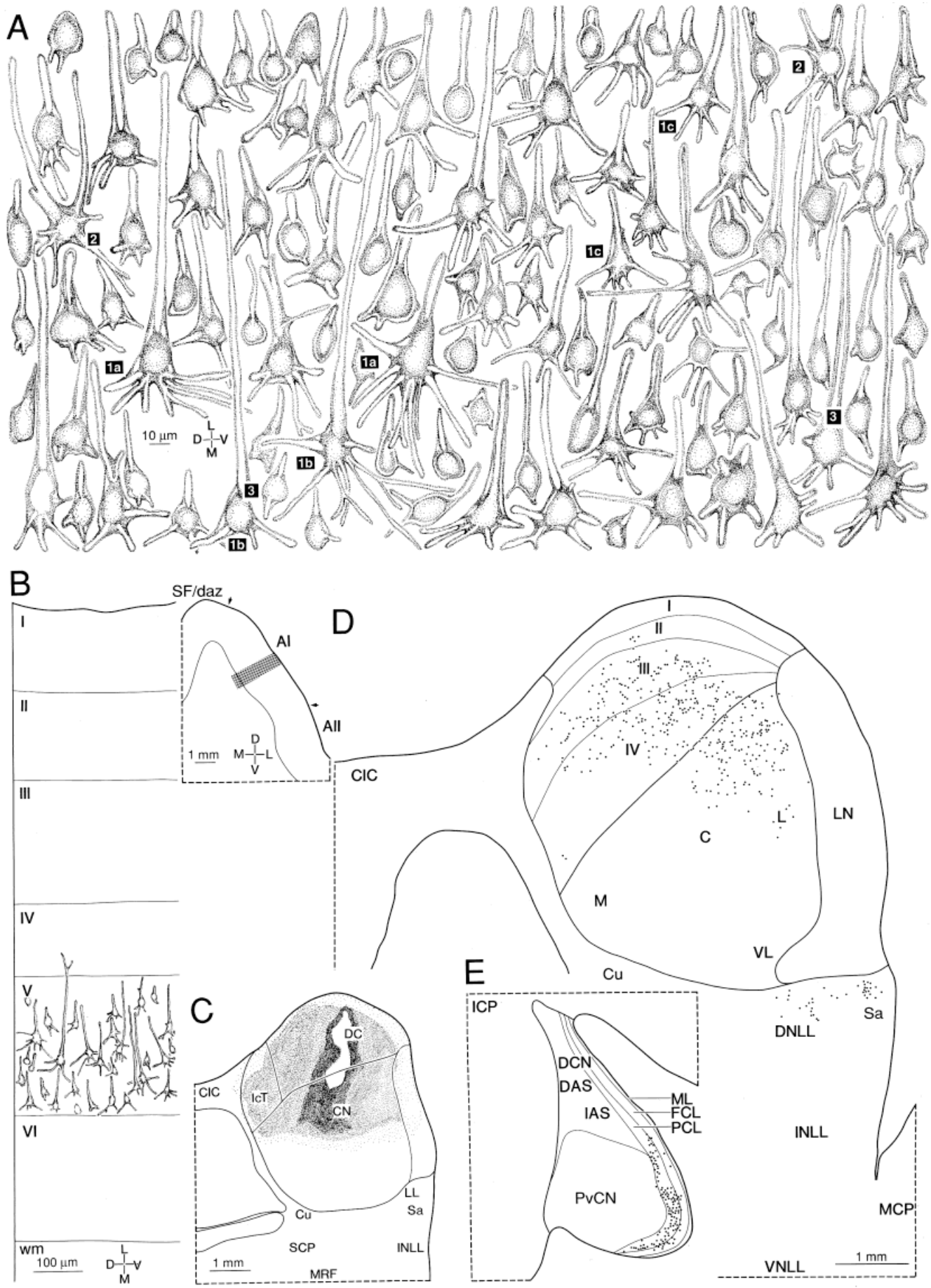
A
2
1c
2
1c
1a
1a
10 µm
L
D
V
M
1b
3
1b
3
B
SF/daz
I
II
III
IV
V
VI
wm
100 µm
AI
AII
1 mm
CIC
C
DC
CIC
IcT
CN
LL
Cu
Sa
SCP
INLL
1 mm
MRF
D
I
II
III
IV
L
LN
C
M
VL
Cu
Sa
DNLL
INLL
MCP
VNLL
1 mm
E
ICP
DCN
DAS
IAS
ML
FCL
PCL
PvCN

Figure 16

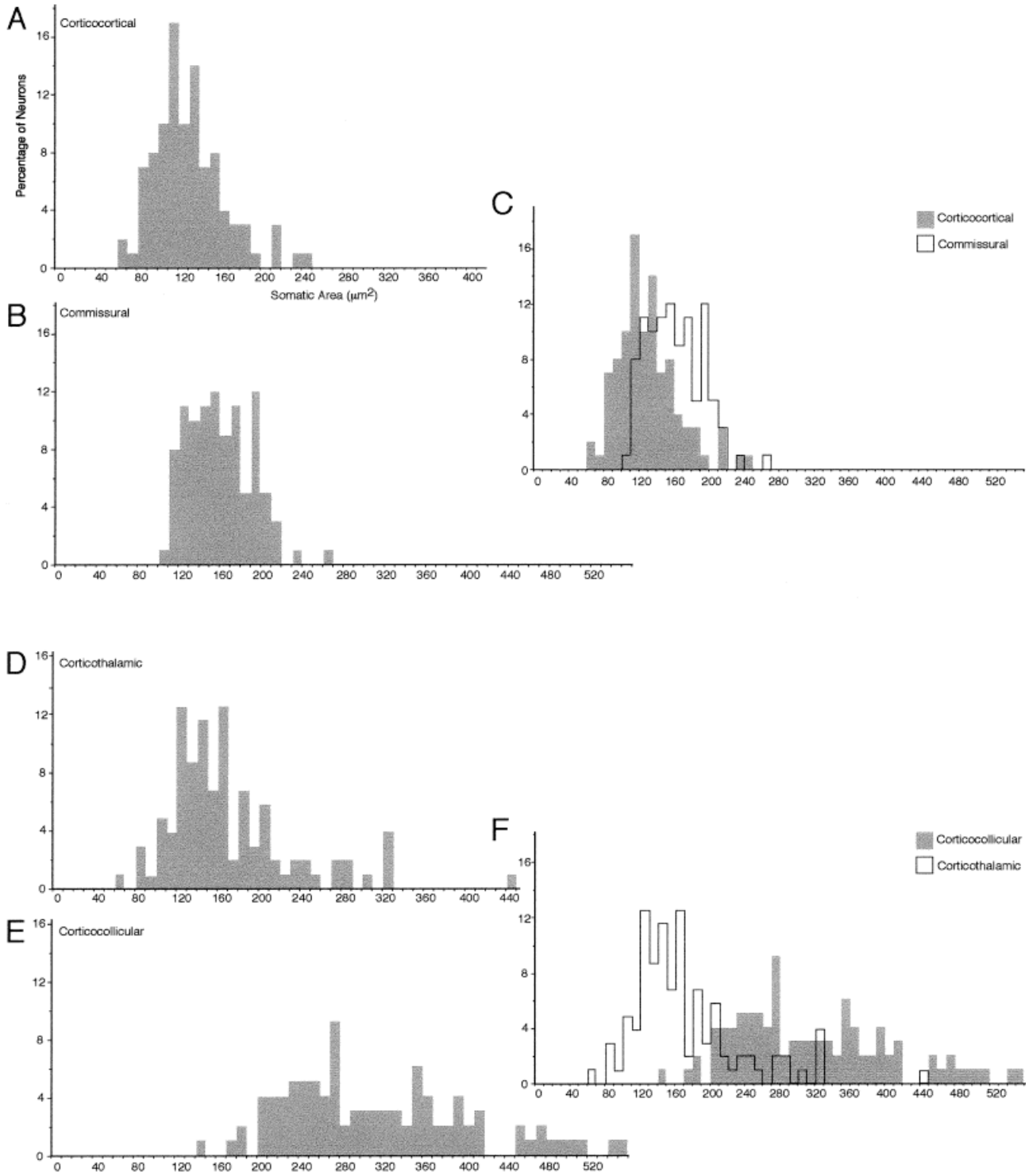


Fig. 17. Somatic size comparison of layer V neurons in AI projecting in the corticocortical (A), commissural (B), corticothalamic (D), and corticocollicular (E) pathways. Statistical comparisons in Table 2 used a sample of 100 well-labeled cells chosen randomly from those in Figures 13A–16A. **A:** Corticocortical cells. **B:** Commissural cells. **C:** The somatic size distribution of corticocortical and commissural cells showed a significant difference. **D:** Corticothalamic cells. **E:** Corticocollicular cells. **F:** Corticothalamic and corticocollicular neurons differed significantly in somatic sizes.

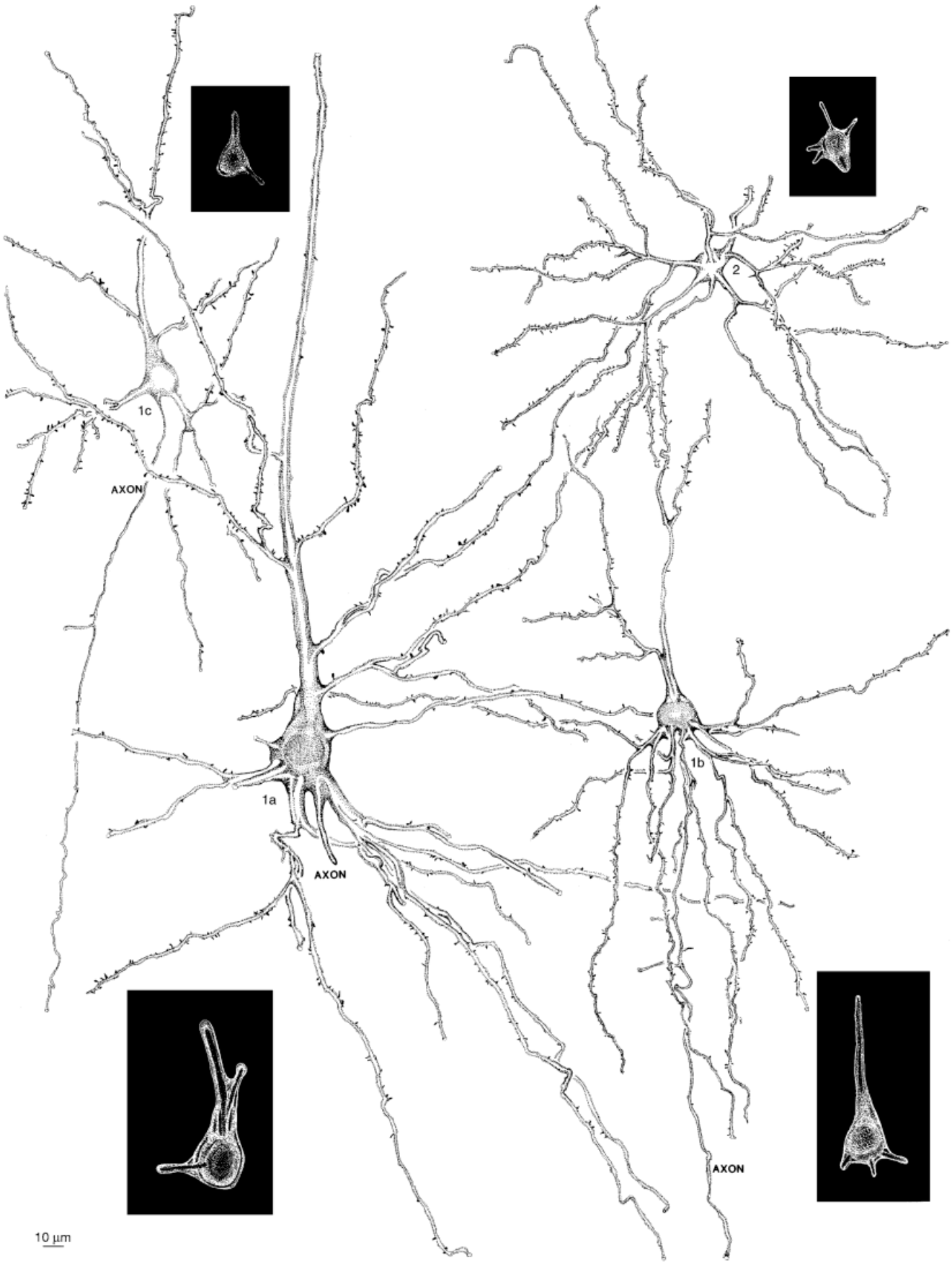


Figure 18

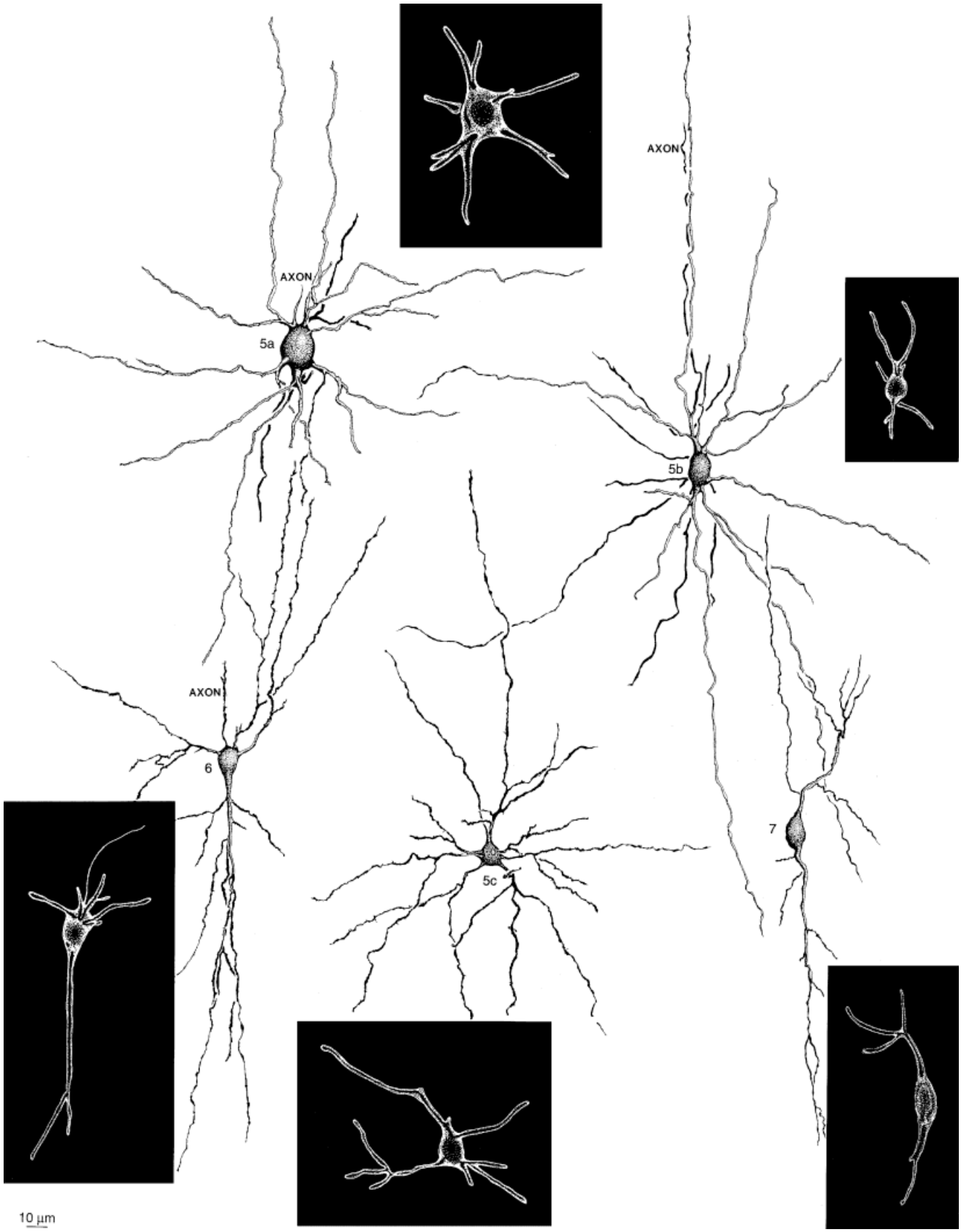


Figure 19

mary visual cortex, association projections to extrastriate cortex included classic large pyramidal cells, with apical dendrites that reach layer I, and inverted and star pyramidal cells (Einstein and Fitzpatrick, 1991). Other layer V large pyramids project only to the superior colliculus (Vogt Weisenhorn et al., 1995). Thus, while large pyramidal neurons are not strictly corticotectal cells, they do not participate equally in all corticocortical connections. These data suggest that (1) the correlation between cell morphology, laminar position, and extracortical target is highly specific; and (2) a cell type may participate in more than one connection, with the proviso that functional subclasses could target different postsynaptic sites. Finally, (3) the intracortical projections support the sublaminar partition of layer V proposed here.

Studies of layer V pyramidal cells in rat somatosensory and visual cortices, in vitro, find a close correspondence between a cell's morphology and intrinsic membrane properties (Chagnac-Amitai et al., 1990). Cells were intrinsically bursting or regular spiking. Bursting cells have a large soma and an apical dendrite that reached layer I (like AI large pyramidal cells), whereas the latter resembled AI medium pyramidal cells. The intrinsic membrane properties of these two types of cells are not mediated by different concentrations of axosomatic synapses (White et al., 1994). Layer V pyramidal cells in rat auditory cortex with intrinsic bursting have less $GABA_A$ input than regular spiking pyramids (Hefti and Smith, 2000). How these physiologic/pharmacologic categories align with the results from Golgi studies is unknown.

Limited data are available on layer V intracortical connections. In cat visual cortex, some layer V cells project to layer VI (Gilbert and Wiesel, 1979) and may contribute to their large receptive fields, because cells with similar orientation selectivity but slightly different receptive field positions converge onto single postsynaptic layer VI cells. Physiologic and anatomic study of layer V large pyramidal cells shows that the projection to layer VI is patchy, partly follows the iso-orientation bands described in the visual cortex (Gabbott et al., 1987), and that it is excitatory. Perhaps such cells in AI with a similar intracortical axonal distribution modulate cells outside their sharpest tuning, or play a role in multipeaked tuning curves (Sutter and Schreiner, 1995), or enhance the several nonuniform representations of frequency (Merzenich et al., 1975), aurality (Imig and Adrián, 1977), amplitude (Schreiner and Urbas, 1988), and breadth of tuning (Sutter and Schreiner, 1991) in AI.

## Speculations on pyramidal cell diversity

Diversity in pyramidal cell dendritic architecture may offer clues to functions. Thus, the apical dendrites should receive these inputs: in layer I, thalamic afferents (Killackey and Ebner, 1972) and GABAergic synapses from Martinotti cells (Marín-Padilla, 1984; Prieto et al., 1994a,b); in layer II, corticocortical (Fisken et al., 1975) and intrinsic (Matsubara and Phillips, 1988) projections; in layer III, thalamic (Hendry and Jones, 1980) and commissural (Code and Winer, 1986) input; in layer IV, thalamic terminals (Pandya and Rosene, 1993); in layer V, weak specific thalamic (Huang and Winer, 2000), modest commissural (Winer, 1992), and axosomatic GABAergic (Prieto et al., 1994b) input. The long, sparsely branched apical dendrite could require close temporal coordination across the many convergent inputs to alter pyramidal cell excitability. In contrast the inputs to basal dendrites may differ greatly. Perhaps the more branched basal system has more $Ca^{2+}$ channels at dendritic nodes (Eilers et al., 1995) for signal amplification, thus requiring less precise afferent input in the temporal domain to elicit a response. The distribution of $GABA_A$ and $GABA_B$ receptors might also contribute to physiologic subtypes in rat auditory cortex (Hefti and Smith, 2000). Pyramidal cells are concurrent members of microcolumnar systems ($<50$ μm wide) with potential high spatial and temporal resolution in signal analysis via their apical dendritic system, and members of a sublaminar network with lower thresholds and coarser macrocolumnar ($>50$–$500$ μm) integrative properties that are embodied by the basal dendritic system.

Nonspecific projections to layer VI (Killackey and Ebner, 1972) might target the inferior dendrites, whereas specific layer IV thalamic afferents (Sousa-Pinto, 1973a,b; Huang and Winer, 2000) end on the superior processes. This could enable two forms of monosynaptic thalamic access to layer V neurons, which have direct thalamic input to their apical dendrites (White and Keller, 1989).

This view considers pyramidal cell function from a perspective of afferent input and largely ignores the signals that they might send to their subcortical targets (Diamond et al., 1992). The microcolumnar system may, thus, produce a focal and topographic effect. In contrast, activation of the basal macrocolumnar system could recruit many more corticothalamic neurons (Contreras et al., 1996) with broader territorial effects on their downstream targets. The patterns of input to large pyramidal (and perhaps other types of) cells and their dendritic geometry might explain how neocortical columnar arrangements influence subcortical neurons. This impact spans a functional domain as fine as the modulation of single neuron receptive fields (Villa et al., 1991) and as global as changes in vigilance (Steriade, 1995).

Fig. 18. (See page 406) Layer V pyramidal neurons include large (1a), medium (1b), small (1c), and star pyramidal (2) cells. Each class differed in size, shape, and sublaminar location. Thus, only the large pyramidal cell had an apical dendrite that reached layer I, and this cell lies in layer Va,b; most of the other types occur throughout layer V. The classic pyramidal cells (1a–c) had similar branching patterns, dendritic appendages, and a common projection scheme for their intrinsic (but not their corticofugal) axons. Medium pyramidal cells often had robust basal arbors, while small pyramidal cells had few dendritic tufts. This finding may relate to different patterns of afferent input (see Discussion section). Star pyramidal cells (2) were not oriented; a principal dendrite projected toward the pia. Black insets, Glutamate-immunoreactive examples of each neuronal type. The inverted pyramidal cell (Fig. 9: 4) is not shown. Protocol for Figures 18, 19: Planapochromat, N.A. 1.32, ×2,000.

Fig. 19. (See previous page) Layer V nonpyramidal neurons: large (5a), medium (5b), and small (5c) multipolar cells were numerous, followed by the Martinotti (6; Fig. 9: 6) and bipolar (7; Fig. 12: 7) neurons. The many types of nonpyramidal neurons aligns layer V with all other layers but I and II, whose neuronal populations are unique (Prieto et al., 1994a). The large multipolar neuron dendritic fields are as large as those of the medium type, and all the multipolar cells had a similar configuration. Bipolar neurons were less tufted than those in layers III (Winer, 1984c) and IV (Winer, 1984a) in AI. Black insets, GAD-immunoreactive examples of each neuronal type.

TABLE 3. Layer V Neurons in AI and in Other Areas and Species[1]

| | | Concordance with Golgi studies or with intracellularly injected cortical neurons | | | | |
|---|---|---|---|---|---|---|
| Neuronal type | Subtypes | Study | Species | Area | Denomination | Figure/s |
| 1. Pyramidal cell | a. Large | Ramón y Cajal, 1899a | Human | Visual | Giant pyramid | 3: F |
| | | Ramón y Cajal, 1899b | Cat | Visual | Giant pyramid | 18: a |
| | | Ramón y Cajal, 1899c | Human | Postcentral gyrus | Giant pyramid | 23 |
| | | Ramón y Cajal, 1899c | Human | Motor | Giant pyramid | 24 |
| | | Ramón y Cajal, 1900 | Human | Auditory | Large pyramid | 7: h |
| | | Ramón y Cajal, 1900 | Human | Sphenoidal (auditory) | Giant pyramid | 16: F,G |
| | | Globus and Scheibel, 1967 | Rabbit | — | Pyramid | 1: 5 |
| | | Tunturi, 1971 | Dog | Auditory | Large pyramid | Table 1: LRG |
| | | Parnavelas et al., 1977 | Rat | Visual | Large pyramidal | 11 |
| | | Parnavelas et al., 1977 | Rat | Visual | Pyramidal | 18a |
| | | Vogt and Peters, 1981 | Rat | Cingulate | Large pyramid | 5: n |
| | | Mitani et al., 1985 | Cat | Auditory | Pyramidal | 11, 12A,C |
| | | Valverde, 1986 | Hedgehog | Postcentralis | Pyramidal | 4: v |
| | | | Cat | Visual | Pyramidal | 5: d |
| | | Van Brederode and Snyder, 1992 | Rat | Sensorimotor | Large pyramidal | 7H |
| | | Fitzpatrick and Henson, 1994 | Bat | Auditory | Pyramidal | 2: M |
| | b. Medium | Ramón y Cajal, 1899b | Cat | Visual | Medium pyramid | 18: b |
| | | Ramón y Cajal, 1921 | Cat | Visual | Pyramid | 11: B, D–G |
| | | Globus and Scheibel, 1967 | Rabbit | — | Pyramid | 1: 4 |
| | | Tunturi, 1971 | Dog | Auditory | Medium sized pyramid | Table 1: MED |
| | | Parnavelas et al., 1977 | Rat | Visual | Pyramidal | 18b |
| | | Mitani et al., 1985 | Cat | Auditory | Pyramidal | 12B |
| | | Valverde, 1986 | Hedgehog | Postcentralis | Pyramidal | 4: u |
| | | | Monkey | Superior temporal sulcus | Pyramidal | 6: o |
| | | Fitzpatrick and Henson, 1994 | Bat | Auditory | Pyramidal | 2: K |
| | c. Small | Ramón y Cajal, 1899a | Human | Visual | Small pyramid | 3: G |
| | | Ramón y Cajal, 1899b | Cat | Visual | Pyramid | 18: d |
| | | Tunturi, 1971 | Dog | Auditory | Small pyramid | Table 1: SM |
| | | Parnavelas et al., 1977 | Rat | Visual | Pyramidal | 18c |
| | | Valverde, 1986 | Monkey | Visual | Pyramidal | 7: n |
| | | Fitzpatrick and Henson, 1994 | Bat | Auditory | Pyramidal | 2: N |
| 2. Star pyramidal cell | — | Ramón y Cajal, 1899c | Human | Precentral gyrus | Pyramid with bifurcated shaft | 12: A (left) |
| | | Ramón y Cajal, 1900 | Human | Auditory | Large polygonal cell | 11: C |
| 3. Fusiform pyramidal cell | — | Ramón y Cajal, 1899b | Cat | Visual | Fusiform cell | 18: m |
| | | Ramón y Cajal, 1900 | Human | Auditory | Small fusiform | 11: I |
| | | Globus and Scheibel, 1967 | Rabbit | — | Spindle | 7: 3 |
| | | Tunturi, 1971 | Dog | Auditory | Fusiform | Table 1: F |
| 4. Inverted pyramidal cell | — | Ramón y Cajal, 1900 | Human | Sphenoidal (auditory) | Cell with descending axon | 16: K |
| | | Ramón y Cajal, 1900 | Cat | Sphenoidal (auditory) | Cell devoid of an apical dendritic shaft | 17: F–J |
| | | Globus and Scheibel, 1967 | Rabbit | — | Inverted pyramid | 2: 1,3,5,8 |
| | | Tunturi, 1971 | Dog | Auditory | Special auditory cell | Table 1: SPECIAL |
| | | Parnavelas et al., 1977 | Rat | Visual | Inverted pyramidal | 3 |
| | | Parnavelas et al., 1977 | Rat | Visual | Inverted pyramidal | 13a,b |
| | | Miller, 1988 | Rat | Visual | Atypically oriented pyramidal | 3: d |
| 5. Multipolar cell | a. Large | Ramón y Cajal, 1899b | Human | Visual | Stellate cell | 19: A,B |
| | | Ramón y Cajal, 1900 | Human | Sphenoidal (auditory) | Large stellate | 16: L |
| | | Jones, 1975 | Monkey | Somatosensory | Type 1 cell | 32 |
| | | Parnavelas et al., 1977 | Rat | Visual | Nonpyramidal | 6b |
| | | Feldman and Peters, 1978 | Rat | Visual | — | 2: c; |
| | | | | | Multipolar | 11: c–e; |
| | | | | | Bitufted | 14: e–g |
| | | | | | Multipolar | 19 |
| | | Peters and Proskauer, 1980 | Rat | Visual | Multipolar | 1: f,g,m,n |
| | | Vogt and Peters, 1981 | Rat | Cingulate | Large multipolar | 5: r; 12: a |
| | | McMullen and Glaser, 1982 | Rabbit | Auditory | Sparsely spined multipolar | 14A |
| | | Meyer, 1983 | Cat | Visual | Multipolar | 13 |
| | | Peters and Kara, 1985 | Rat | Visual | Sparsely spinous bitufted | 9 |
| | | Meyer, 1987 | Human | Motor | Local-axon neuron | 12: 4 |
| | | Lund et al., 1988 | Monkey | Visual | 5B-5 | 6 |
| | | Lund and Lewis, 1993 | Monkey | Prefrontal | Basket neuron | 7 |
| | | Fitzpatrick and Henson, 1994 | Bat | Auditory | Multipolar | 5: M |
| | b. Medium | Ramón y Cajal, 1899b | Human | Visual | Cell with ascending axon | 19: C |
| | | Ramón y Cajal, 1899c | Human | Precentral gyrus | Stellate cell | 18: C,D,E |
| | | Globus and Scheibel, 1967 | Rabbit | — | Stellate | 5: 15 |
| | | Feldman and Peters, 1978 | Rat | Visual | Multipolar | 10: f |
| | | Peters and Proskauer, 1980 | Rat | Visual | Multipolar | 1: f,o,p |
| | | Vogt and Peters, 1981 | Rat | Cingulate | Medium multipolar | 10: a–d |
| | | Meyer, 1987 | Human | Motor | Local-axon neuron | 12: 5 |
| | | Lund et al., 1988 | Monkey | Visual | 5B-4 | 4b, 5 |
| | | Fitzpatrick and Henson, 1994 | Bat | Auditory | Multipolar | 5: N |
| | c. Small | Ramón y Cajal, 1899c | Human | Precentral gyrus | Cell with short axon | 12: D |
| | | Globus and Scheibel, 1967 | Rabbit | — | Stellate | 5: 8,9 |
| | | Vogt and Peters, 1981 | Rat | Cingulate | Medium multipolar | 12: b |
| | | Somogyi et al., 1984 | Monkey | Visual | Small aspiny multipolar | 3: 12 |
| | | Werner et al., 1989 | Monkey | Visual | Neurogliaform | 7E |
| | | Fitzpatrick and Henson, 1994 | Bat | Auditory | Multipolar | 5: K |
| 6. Martinotti cell | — | Ramón y Cajal, 1893 | Rabbit | Occipital | — | 4, t |
| | | Meyer, 1983 | Cat | Visual | Multipolar | 12: a,b |
| | | Lund, 1987 | Monkey | Visual | 5A-4 | 12 |
| | | Meyer, 1987 | Human | Motor | Local-axon neuron | 12: 6 |
| 7. Bipolar cell | — | Ramón y Cajal, 1900 | Human | Auditory | Tiny cell with ascending axon | 11: E,G |
| | | Feldman and Peters, 1978 | Rat | Visual | Bipolar | 15: d |
| | | Peters and Regidor, 1981 | Cat | Visual | Bipolar | 11: S |
| | | Meyer, 1983 | Cat | Visual | Bitufted | 18: a |
| | | Fitzpatrick and Henson, 1994 | Bat | Auditory | Bipolar | 5: L |

[1]—, data not available.

## ACKNOWLEDGMENTS

We thank Mr. David T. Larue for expert assistance with photomicrography. Ms. Pamela Woronoff measured the neurons. Dr. Camillan L. Huang kindly helped with the digital processing of Figure 2.

## LITERATURE CITED

Aitkin LM, Phillips SC. 1984. The interconnections of the inferior colliculi through their commissure. J Comp Neurol 228:210–216.

Aitkin LM, Webster WR. 1972. Medial geniculate body of the cat: organization and responses to tonal stimuli of neurons in ventral division. J Neurophysiol 35:365–380.

Beneyto M, Winer JA, Larue DT, Prieto JJ. 1998. Auditory connections and neurochemical organization of the sagulum. J Comp Neurol 401:329–351.

Berman AL. 1968. The brain stem of the cat: a cytoarchitectonic atlas with stereotaxic coordinates. Madison, WI: University of Wisconsin Press.

Berman AL, Jones EG. 1982. The thalamus and basal telencephalon of the cat. A cytoarchitectonic atlas with stereotaxic coordinates. Madison and London: The University of Wisconsin Press.

Bourassa J, Deschênes M. 1995. Corticothalamic projections from the primary visual cortex in rats: a single fiber study using biocytin as an anterograde tracer. Neuroscience 66:253–263.

Calford MB, Aitkin LM. 1983. Ascending projections to the medial geniculate body of the cat: evidence for multiple, parallel auditory pathways through the thalamus. J Neurosci 3:2365–2380.

Castro-Alamancos MA, Connors BW. 1996. Short-term plasticity of a thalamocortical pathway dynamically modulated by behavioral state. Science 272:274–277.

Chagnac-Amitai Y, Luhmann HJ, Prince DA. 1990. Burst generating and regular spiking layer 5 pyramidal neurons of rat neocortex have different morphological features. J Comp Neurol 296:598–613.

Chan-Palay V, Palay SL, Billings-Gagliardi SM. 1974. Meynert cells in the primate visual cortex. J Neurocytol 3:631–658.

Code RA, Winer JA. 1985. Commissural neurons in layer III of cat primary auditory cortex (AI): pyramidal and non-pyramidal cell input. J Comp Neurol 242:485–510.

Code RA, Winer JA. 1986. Columnar organization and reciprocity of commissural connections in cat primary auditory cortex (AI). Hear Res 23:205–222.

Colwell S. 1975. Thalamocortical-corticothalamic reciprocity: a combined anterograde-retrograde tracer technique. Brain Res 92:443–449.

Contreras D, Destexhe A, Sejnowski TJ, Steriade M. 1996. Control of spatiotemporal coherence of a thalamic oscillation by corticothalamic feedback. Science 274:771–774.

De Carlos JA, Lopez-Mascaraque L, Valverde F. 1985. Development, morphology, and topography of chandelier cells in the auditory cortex of the cat. Brain Res Dev Brain Res 22:293–300.

Diamond IT, Jones EG, Powell TPS. 1969. The projection of the auditory cortex upon the diencephalon and brain stem of the cat. Brain Res 15:305–340.

Diamond ME, Armstrong-James M, Budway MJ, Ebner FF. 1992. Somatic sensory responses in the rostral sector of the posterior group (POm) and in the ventral posterior medial nucleus (VPM) of the rat thalamus: dependence on the barrel field cortex. J Comp Neurol 319:66–84.

Eilers J, Augustine GJ, Konnerth A. 1995. Subthreshold synaptic $Ca^{2+}$ signalling in fine dendrites and spines of cerebellar Purkinje neurons. Nature 373:155–158.

Einstein G, Fitzpatrick D. 1991. Distribution and morphology of area 17 neurons that project to the cat's extrastriate cortex. J Comp Neurol 303:132–149.

Fariñas I, DeFelipe J. 1991a. Patterns of synaptic input on corticocortical and corticothalamic cells in the cat visual cortex. I. The cell body. J Comp Neurol 304:53–69.

Fariñas I, DeFelipe J. 1991b. Patterns of synaptic input on corticocortical and corticothalamic cells in the cat visual cortex. II. The axon initial segment. J Comp Neurol 304:70–77.

Feldman ML, Peters A. 1978. The forms of non-pyramidal neurons in the visual cortex of the rat. J Comp Neurol 179:761–794.

Ferster D, Lindström S. 1985. Augmenting responses evoked in area 17 of the cat by intracortical axon collaterals of cortico-geniculate cells. J Physiol (Lond) 367:217–232.

Fisken RA, Garey LJ, Powell TPS. 1975. The intrinsic, association and commissural connections of area 17 of the visual cortex. Philos Trans R Soc Lond B 272:487–536.

Fitzpatrick D, Usrey WM, Schofield BR, Einstein G. 1994. The sublaminar organization of corticogeniculate neurons in layer 6 of macaque striate cortex. Vis Neurosci 11:307–315.

Fitzpatrick DC, Henson OW. 1994. Cell types in the mustached bat auditory cortex. Brain Behav Evol 43:79–91.

Flaherty AW, Graybiel AM. 1995. Motor somatosensory corticostriatal projection magnifications in the squirrel monkey. J Neurophysiol 74:2638–2648.

Gabbott PLA, Martin KAC, Whitteridge D. 1987. Connections between pyramidal neurons in layer 5 of cat visual cortex. J Comp Neurol 259:364–381.

Games KD, Winer JA. 1988. Layer V in rat auditory cortex: projections to the inferior colliculus and contralateral cortex. Hear Res 34:1–26.

Gilbert CD, Wiesel TN. 1979. Morphology and intracortical projections of functionally characterised neurones in the cat visual cortex. Nature 280:120–125.

Globus A, Scheibel AB. 1967. Pattern and field in cortical structure: the rabbit. J Comp Neurol 131:155–172.

Hallman EL, Schofield BR, Lin C-S. 1988. Dendritic morphology and axon collaterals of corticotectal, corticopontine, and callosal neurons in layer V of primary visual cortex of the hooded rat. J Comp Neurol 272:149–160.

Hefti BJ, Smith P. 2000. Anatomy, physiology, and synaptic responses of rat layer V auditory cortical cells and effects of intracellular $GABA_A$ blockade. J Neurophysiol 83:2626–2638.

Hendry SHC, Jones EG. 1980. Electron microscopic demonstration of thalamic axon terminations on identified commissural neurons in monkey somatic sensory cortex. Brain Res 196:253–257.

Hendry SHC, Schwark HD, Jones EG, Yan J. 1987. Numbers and proportions of GABA-immunoreactive neurons in different areas of monkey cerebral cortex. J Neurosci 7:1503–1519.

Henkel CK. 1983. Evidence of sub-collicular auditory projections to the medial geniculate nucleus in the cat: an autoradiographic and horseradish peroxidase study. Brain Res 259:21–30.

Huang CL, Winer JA. 2000. Auditory thalamocortical projections in the cat: laminar and areal patterns of input. J Comp Neurol 427:302–331.

Hubel DH, Wiesel TN. 1972. Laminar and columnar distribution of geniculo-cortical fibers in the macaque monkey. J Comp Neurol 146:421–450.

Hübener M, Bolz J. 1992. Relationships between dendritic morphology and cytochrome oxidase compartments in monkey striate cortex. J Comp Neurol 324:67–80.

Hübener M, Schwarz C, Bolz J. 1990. Morphological types of projection neurons in layer 5 of cat visual cortex. J Comp Neurol 301:655–674.

Huettner JE, Baughman RW. 1988. The pharmacology of synapses formed by identified corticocollicular neurons in primary cultures of rat visual cortex. J Neurosci 8:160–175.

Huffman RF, Henson OW Jr. 1990. The descending auditory pathway and acousticomotor systems: connections with the inferior colliculus. Brain Res Brain Res Rev 15:295–323.

Imig TJ, Adrián HO. 1977. Binaural columns in the primary auditory field (A1) of cat auditory cortex. Brain Res 138:241–257.

Imig TJ, Morel A. 1984. Topographic and cytoarchitectonic organization of thalamic neurons related to their targets in low-, middle-, and high-frequency representations in cat auditory cortex. J Comp Neurol 227:511–539.

Imig TJ, Morel A, Kauer CD. 1982. Covariation of distribution of callosal cell bodies and callosal axon terminals in layer III of cat primary auditory cortex. Brain Res 251:157–159.

Jones EG. 1975. Varieties and distribution of non-pyramidal cells in the somatic cortex of the squirrel monkey. J Comp Neurol 160:205–268.

Jones EG, Wise SP. 1977. Size, laminar and columnar distribution of efferent cells in the sensory-motor cortex of monkeys. J Comp Neurol 175:391–438.

Jones EG, Coulter JD, Burton H, Porter R. 1977. Cells of origin and terminal distribution of corticostriatal fibers arising in the sensory-motor cortex of monkeys. J Comp Neurol 173:53–80.

Katz LC. 1987. Local circuitry of identified projection neurons in cat visual cortex brain slices. J Neurosci 7:1223–1249.

Kelly JP, Wong D. 1981. Laminar connections of the cat's auditory cortex. Brain Res 212:1–15.

Kilgard MP, Merzenich MM. 1998. Cortical map reorganization enabled by nucleus basalis activity. Science 279:1714–1718.

Killackey HP, Ebner FF. 1972. Two different types of thalamocortical projections to a single cortical area in mammals. Brain Behav Evol 6:141–169.

Killackey HP, Koralek K-A, Chiaia NL, Rhoades RW. 1989. Laminar and areal differences in the origin of the subcortical projection neurons of the rat somatosensory cortex. J Comp Neurol 282:428–445.

King AJ. 1995. Asking the auditory cortex the right question. Curr Biol 5:1110–1113.

Kisvárday Z, Beaulieu C, Eysel U. 1993. Network of GABAergic large basket cells in cat visual cortex (area 18): implication for lateral disinhibition. J Comp Neurol 327:398–415.

Kisvárday ZF, Cowey A, Hodson AJ, Somogyi P. 1986. The relationship between GABA immunoreactivity and labelling by local uptake of [$^3$H] GABA in the striate cortex of monkey. Exp Brain Res 62:89–98.

Knudsen EI, Brainard MS. 1995. Creating a unified representation of visual and auditory space in the brain. Annu Rev Neurosci 18:19–43.

Kuypers HGJM, Lawrence DG. 1967. Cortical projections to the red nucleus and the brain stem in the rhesus monkey. Brain Res 4:151–188.

Larue DT, Winer JA. 1996. Postembedding immunocytochemistry of large sections of brain tissue: an improved flat-embedding technique. J Neurosci Methods 68:125–132.

Lévesque M, Charara A, Gagnon S, Parent A, Deschênes M. 1996a. Corticostriatal projections from layer V cells in rat are collaterals of long-range corticofugal axons. Brain Res 709:311–315.

Lévesque M, Gagnon S, Parent A, Deschênes M. 1996b. Axonal arborizations of corticostriatal and corticothalamic fibers arising from the second somatosensory area in the rat. Cereb Cortex 6:759–770.

Lorente de Nó R. 1938. Architectonics and structure of the cerebral cortex. In: Fulton JF, editor. Physiology of the nervous system. London: Oxford University Press. p 291–330.

Lübke J, Markram H, Frotscher M, Sakmann B. 1996. Frequency and dendritic distribution of autapses established by layer 5 pyramidal neurons in the developing rat neocortex: comparison with synaptic innervation of adjacent neurons of the same class. J Neurosci 16:3209–3218.

Lund JS. 1973. Organization of neurons in the visual cortex, area 17, of the monkey (*Macaca mulatta*). J Comp Neurol 147:455–496.

Lund JS. 1987. Local circuit neurons of macaque monkey striate cortex: I. Neurons of laminae 4C and 5A. J Comp Neurol 257:60–92.

Lund JS, Lewis DA. 1993. Local circuit neurons of developing and mature macaque prefrontal cortex: Golgi and immunocytochemical characteristics. J Comp Neurol 328:282–312.

Lund JS, Hawken MJ, Parker AJ. 1988. Local circuit neurons of macaque monkey striate cortex: II. Neurons of laminae 5B and 6. J Comp Neurol 276:1–29.

Madl JE, Beitz AJ, Johnson RL, Larson AA. 1987. Monoclonal antibodies specific for fixative-modified aspartate: immunocytochemical localization in the rat CNS. J Neurosci 7:2639–2650.

Marín-Padilla M. 1984. Neurons of layer I. A developmental analysis. In: Peters A, Jones EG, editors. Cerebral cortex, vol. 1, Cellular components of the cerebral cortex, New York, New York, Plenum Press p 447–478.

Matsubara JA, Phillips DP. 1988. Intracortical connections and their physiological correlates in the primary auditory cortex (AI) of the cat. J Comp Neurol 268:38–48.

McMullen NT, Glaser EM. 1982. Morphology and laminar distribution of nonpyramidal neurons in the auditory cortex of the rabbit. J Comp Neurol 208:85–106.

Merzenich MM, Reid MD. 1974. Representation of the cochlea within the inferior colliculus of the cat. Brain Res 77:397–415.

Merzenich MM, Knight PL, Roth GL. 1975. Representation of cochlea within primary auditory cortex in the cat. J Neurophysiol 38:231–249.

Mesulam M-M. 1978. Tetramethyl benzidine for horseradish peroxidase neurohistochemistry: a non-carcinogenic blue reaction-product with superior sensitivity for visualizing neural afferents and efferents. J Histochem Cytochem 26:106–117.

Meyer G. 1983. Axonal patterns and topography of short-axon neurons in visual areas 17, 18, and 19 of the cat. J Comp Neurol 220:405–438.

Meyer G. 1987. Forms and spatial arrangement of neurons in the primary motor cortex of man. J Comp Neurol 262:402–428.

Meyer G, Albus K. 1981. Spiny stellates as cells of origin of association fibres from area 17 to area 18, in the cat's neocortex. Brain Res 210: 335–341.

Miller MW. 1988. Maturation of rat visual cortex: IV. The generation, migration, morphogenesis, and connectivity of atypically oriented pyramidal neurons. J Comp Neurol 274:387–405.

Mitani A, Shimokouchi M, Itoh K, Nomura S, Kudo M, Mizuno N. 1985. Morphology and laminar organization of electrophysiologically identified neurons in primary auditory cortex in the cat. J Comp Neurol 235:430–447.

Morest DK. 1965. The lateral tegmental system of the midbrain and the medial geniculate body: study with Golgi and Nauta methods in cat. J Anat (Lond.) 99:611–634.

Morest DK, Oliver DL. 1984. The neuronal architecture of the inferior colliculus in the cat: defining the functional anatomy of the auditory midbrain. J Comp Neurol 222:209–236.

Moriizumi T, Hattori T. 1991. Pyramidal cells in rat temporoauditory cortex project to both striatum and inferior colliculus. Brain Res Bull 27:141–144.

Nicoll A, Blakemore C. 1993. Single-fibre EPSPs in layer 5 of rat visual cortex in vitro. Neuroreport 4:167–170.

Niimi K, Matsuoka H. 1979. Thalamocortical organization of the auditory system in the cat studied by retrograde axonal transport of horseradish peroxidase. Adv Anat Embryol Cell Biol 57:1–56.

Ojima H. 1994. Terminal morphology and distribution of corticothalamic fibers originating from layers 5 and 6 of cat primary auditory cortex. Cereb Cortex 6:646–663.

Ojima H, Honda CN, Jones EG. 1992. Characteristics of intracellularly injected infragranular pyramidal neurons in cat primary auditory cortex. Cereb Cortex 2:197–216.

Oliver DL. 1984. Dorsal cochlear nucleus projections to the inferior colliculus in the cat. A light and electron microscopic study. J Comp Neurol 224:155–172.

Pandya DN, Rosene DL. 1993. Laminar termination patterns of thalamic, callosal, and association afferents in the primary auditory area of the rhesus monkey. Expl Neurol 119:220–234.

Parnavelas JG, Lieberman AR, Webster KE. 1977. Organization of neurons in the visual cortex, area 17, of the rat. J Anat 124:305–322.

Peters A, Kara DA. 1985. The neuronal composition of area 17 of rat visual cortex: II. The nonpyramidal cells. J Comp Neurol 234:242–263.

Peters A, Proskauer CC. 1980. Smooth or sparsely spined cells with myelinated axons in rat visual cortex. Neuroscience 5:2079–2092.

Peters A, Regidor J. 1981. A reassessment of the forms of nonpyramidal neurons in area 17 of cat visual cortex. J Comp Neurol 203:685–716.

Peters A, Sethares C. 1996. Myelinated axons and the pyramidal cell modules in monkey primary visual cortex. J Comp Neurol 365:232–255.

Phillips CG, Porter R. 1977. Corticospinal neurones. Their role in movement. London: Academic Press.

Prieto JJ, Winer JA. 1999. Neurons of layer VI in cat primary auditory cortex (AI): Golgi study and sublaminar origins of projection neurons. J Comp Neurol 404:332–358.

Prieto JJ, Peterson BA, Winer JA. 1994a. Morphology and spatial distribution of GABAergic neurons in cat primary auditory cortex (AI). J Comp Neurol 344:349–382.

Prieto JJ, Peterson BA, Winer JA. 1994b. Laminar distribution and neuronal targets of GABAergic axon terminals in cat primary auditory cortex (AI). J Comp Neurol 344:383–402.

Ramón-Moliner E. 1970. The Golgi-Cox technique. In: Nauta WJH, Ebbesson SOE, editors. Contemporary research methods in neuroanatomy. Heidelberg: Springer-Verlag, p 32–55.

Ramón y Cajal S. 1893. Estructura de la corteza occipital inferior de los pequeños mamíferos. Anal Soc Española Historia Nat 22:115–125.

Ramón y Cajal S. 1899a. Apuntes para el estudio estructural de la corteza visual del cerebro humano. Rev Ibero-Americana Cienc Méd 1:1–14.

Ramón y Cajal S. 1899b. Estudios sobre la corteza cerebral humana I: corteza visual. Rev trim Micrográf, Madrid, 4:1–63.

Ramón y Cajal S. 1899c. Estudios sobre la corteza cerebral humana II: Estructura de la corteza motriz del hombre y mamíferos superiores. Rev trim Micrográf, Madrid, 4:117–200.

Ramón y Cajal S. 1900. Estudios sobre la corteza cerebral humana III: Corteza acústica. Rev trim Micrográf, Madrid, 5:129–183.

Ramón y Cajal S. 1921. Textura de la corteza visual del gato. Arch Neurobiol, Madrid, 2:338–362.

Reale RA, Imig TJ. 1983. Auditory cortical field projections to the basal ganglia of the cat. Neuroscience 8:67–86.

Rose JE. 1949. The cellular structure of the auditory region of the cat. J Comp Neurol 91:409–440.

Schofield BR, Hallman LE, Lin C-S. 1987. Morphology of corticotectal cells in the primary visual cortex of hooded rats. J Comp Neurol 261:85–97.

Schreiner CE, Urbas JV. 1988. Representation of amplitude modulation in the auditory cortex of the cat: II. Comparison between cortical fields. Hear Res 32:49–64.

Society for Neuroscience. 1991. Handbook for the use of animals in neuroscience research. Washington, DC: Society for Neuroscience.

Somogyi P, Kisvárday ZF, Freund TF, Cowey A. 1984. Characterization by Golgi impregnation of neurons that accumulate $^{3}$H-GABA in the visual cortex of monkey. Exp Brain Res 53:295–303.

Sousa-Pinto A. 1973a. Cortical projections of the medial geniculate body in the cat. Adv Anat Embryol Cell Biol 48:1–42.

Sousa-Pinto A. 1973b. The structure of the first auditory cortex (A I) in the cat — I. Light microscopic observations on its structure. Arch Ital Biol 111:112–137.

Spirou GA, May BJ, Wright DD, Ryugo DK. 1993. Frequency organization of the dorsal cochlear nucleus in cats. J Comp Neurol 329:36–52.

Staiger JF, Zilles K, Freund TF. 1996. Recurrent axon collaterals of corticothalamic projection neurons in rat primary somatosensory cortex contribute to excitatory and inhibitory feedback-loops. Anat Embryol (Berl) 194:533–543.

Steriade M. 1995. Brain activation, then (1949) and now: coherent fast rhythms in corticothalamic networks. Arch Ital Biol 134:5–20.

Stevens CF. 1998. Neuronal diversity: too many cell types for comfort? Curr Biol 8:R708–R710.

Sutter ML, Schreiner CE. 1991. Physiology and topography of neurons with multipeaked tuning curves in cat primary auditory cortex. J Neurophysiol 65:1207–1226.

Sutter ML, Schreiner CE. 1995. Topography of intensity tuning in cat primary auditory cortex: single-neuron versus multiple-neuron recordings. J Neurophysiol 73:190–204.

Tunturi AR. 1971. Classification of neurons in the ectosylvian auditory cortex of the dog. J Comp Neurol 142:153–166.

Valverde F. 1986. Intrinsic neocortical organization: some comparative aspects. Neuroscience 18:1–23.

Van Brederode JFM, Snyder GL. 1992. A comparison of the electrophysiological properties of morphologically identified cells in layers 5B and 6 of the rat neocortex. Neuroscience 50:315–337.

Villa AEP, Rouiller EM, Simm GM, Zurita P, de Ribaupierre Y, de Ribaupierre F. 1991. Corticofugal modulation of the information processing in the auditory thalamus of the cat. Exp Brain Res 86:506–517.

Vogt BA, Peters A. 1981. Form and distribution of neurons in rat cingulate cortex: areas 32, 24, and 29. J Comp Neurol 195:603–625.

Vogt Weisenhorn DM, Illing R-B, Spatz WB. 1995. Morphology and connections of neurons in area 17 projecting to the extrastriate areas MT and 19DM and to the superior colliculus in the monkey *Callithrix jacchus*. J Comp Neurol 362:233–255.

von Economo C. 1929. The cytoarchitectonics of the human cerebral cortex. London: Oxford University Press and Humphrey Milford.

Weedman DL, Ryugo DK. 1996a. Projections from auditory cortex to the cochlear nucleus in rats: synapses on granule cell dendrites. J Comp Neurol 371:311–324.

Weedman DL, Ryugo DK. 1996b. Pyramidal cells in primary auditory cortex project to cochlear nucleus in rat. Brain Res 706:97–102.

Weinberger NM. 1997. Learning-induced receptive field plasticity in the auditory cortex. Semin Neurosci 9:59–67.

Werner L, Winkelmann E, Koglin A, Neser J, Rodewohl H. 1989. A Golgi deimpregnation study of neurons in the rhesus monkey visual cortex (areas 17 and 18). Anat Embryol (Berl) 180:583–597.

White EL, Keller A. 1989. Cortical circuits. Synaptic organization of the cerebral cortex. Structure, function, and theory. Boston, MA: Birkhäuser.

White EL, Amitai Y, Gutnick MJ. 1994. A comparison of synapses onto the somata of intrinsically bursting and regular spiking neurons in layer V of rat SmI cortex. J Comp Neurol 342:1–14.

Winer JA. 1984a. Anatomy of layer IV in cat primary auditory cortex (AI). J Comp Neurol 224:535–567.

Winer JA. 1984b. The pyramidal cells in layer III of cat primary auditory cortex (AI). J Comp Neurol 229:476–496.

Winer JA. 1984c. The non-pyramidal neurons in layer III of cat primary auditory cortex (AI). J Comp Neurol 229:512–530.

Winer JA. 1985. Structure of layer II in cat primary auditory cortex (AI). J Comp Neurol 238:10–37.

Winer JA. 1992. The functional architecture of the medial geniculate body and the primary auditory cortex. In: Webster DB, Popper AN, Fay RR, editors. Springer handbook of auditory research, Vol. 1, the mammalian auditory pathway: neuroanatomy. New York, New York: Springer-Verlag, p 222–409.

Winer JA, Larue DT. 1989. Populations of GABAergic neurons and axons in layer I of rat auditory cortex. Neuroscience 33:499–515.

Winer JA, Larue DT. 1996. Evolution of GABAergic circuitry in the mammalian medial geniculate body. Proc Natl Acad Sci USA 93:3083–3087.

Winer JA, Larue DT, Diehl JJ, Hefti BJ. 1998. Auditory cortical projections to the cat inferior colliculus. J Comp Neurol 400:147–174.

Winer JA, Larue DT, Huang CL. 1999. Two systems of giant axon terminals in the cat medial geniculate body: convergence of cortical and GABAergic inputs. J Comp Neurol 413:181–197.

Winguth SD, Winer JA. 1986. Corticocortical connections of cat primary auditory cortex (AI): laminar organization and identification of supragranular neurons projecting to area AII. J Comp Neurol 248:36–56.